REPORT DOCUMENTATION PAGE

Form Approved OMB NO. 0704-0188

1. REPORT DATE (DD-MM-YYYY)	2. REPORT TYPE	3. DATES COVERED (From - To)
31-12-2007	Final Report	15-May-2005 - 14-Nov-2007

4. TITLE AND SUBTITLE
New Therapeutic Strategies for Antibiotic-Resistant Select Agents

5a. CONTRACT NUMBER
W911NF-05-1-0275

5b. GRANT NUMBER

5c. PROGRAM ELEMENT NUMBER
5310U4

6. AUTHORS
Steven H. Hinrichs, Mark Griep

5d. PROJECT NUMBER

5e. TASK NUMBER

5f. WORK UNIT NUMBER

7. PERFORMING ORGANIZATION NAMES AND ADDRESSES
University of Nebraska Medical Center
Sponsored Programs Administrat
University of Nebraska Medical Center
Omaha, NE 68198 -7835

8. PERFORMING ORGANIZATION REPORT NUMBER

9. SPONSORING/MONITORING AGENCY NAME(S) AND ADDRESS(ES)
U.S. Army Research Office
P.O. Box 12211
Research Triangle Park, NC 27709-2211

10. SPONSOR/MONITOR'S ACRONYM(S)
ARO

11. SPONSOR/MONITOR'S REPORT NUMBER(S)
48810-LS-DRP.1

12. DISTRIBUTION AVAILIBILITY STATEMENT
Approved for public release; Federal purpose rights

13. SUPPLEMENTARY NOTES
The views, opinions and/or findings contained in this report are those of the author(s) and should not contrued as an official Department of the Army position, policy or decision, unless so designated by other documentation.

14. ABSTRACT
The goal of this project was to establish the scientific basis for a new class of antibiotics that are needed to combat the development of resistance to currently available medications or the engineering of resistance into biological select agents. A multidisciplinary team of microbiologists, biochemists, molecular biologists and drug discovery experts was established to explore the hypothesis that disruption of bacterial primase activity will provide the basis for antimicrobial discovery and further, that the modular components of primase will provide for the discovery of broad- and narrow-spectrum antibiotics. The experimental model examined the functional activities of the Gram positive Staphylococcus aureus with the Gram negative E.

15. SUBJECT TERMS
Final Report

16. SECURITY CLASSIFICATION OF:			17. LIMITATION OF ABSTRACT	15. NUMBER OF PAGES	19a. NAME OF RESPONSIBLE PERSON
a. REPORT	b. ABSTRACT	c. THIS PAGE			Steven Hinrichs
UL	U	U	SAR		19b. TELEPHONE NUMBER 402-559-7203

Report Title

New Therapeutic Strategies for Antibiotic-Resistant Select Agents

ABSTRACT

The goal of this project was to establish the scientific basis for a new class of antibiotics that are needed to combat the development of resistance to currently available medications or the engineering of resistance into biological select agents. A multidisciplinary team of microbiologists, biochemists, molecular biologists and drug discovery experts was established to explore the hypothesis that disruption of bacterial primase activity will provide the basis for antimicrobial discovery and further, that the modular components of primase will provide for the discovery of broad- and narrow-spectrum antibiotics. The experimental model examined the functional activities of the Gram positive Staphylococcus aureus with the Gram negative E. coli for purposes of establishing a protocol for extension to select agents including Bacillus anthracis and Yersinia pestis. Important discoveries that confirmed the potential of this approach included the finding that S. aureus primase synthesized RNA using a different initiation site from that previously found for E. coli, and that helicase stimulation of primase was restricted at the genus level. Results were confirmed with recombinant Y. pestis and B. anthracis proteins. A two prong approach was used to identify chemicals that could serve as compounds leading to a new antimicrobial drug including computational screening of chemical libraries and high throughput screening positioning this work for the next phase of development.

List of papers submitted or published that acknowledge ARO support during this reporting period. List the papers, including journal references, in the following categories:

(a) Papers published in peer-reviewed journals (N/A for none)

Chintakayala K, Larson, MA, Grainger, WH, Scott, DJ, Griep MA, Hinrichs SH, and Soultanas, P. Molecular Microbiology (2007) 63:1629-1639. Domain Swapping Reveals that the C- and N-Terminal Domains of DnaG and DnaB, Respectively, Are Functional Homologues.

Griep MA, Blood S, Larson, MA, Koepsell SA and Hinrichs SH. Bioorganic & Medicinal Chemistry 15 (2007) 7203-7208. Myricetin Inhibits Escherichia coli DnaB helicase but not E coli Primase.

Koepsell SA, Larson MA, Griep MA, and Hinrichs SH. Journal of Bacteriology, July, 2006: 4673-4680. Staphylococcus aureus Helicase but not Escherichia coli Helicase Stimulates S. aureus Primase Activity and Maintains Initiation Specificity

Number of Papers published in peer-reviewed journals: 3.00

(b) Papers published in non-peer-reviewed journals or in conference proceedings (N/A for none)

Number of Papers published in non peer-reviewed journals: 0.00

(c) Presentations

Number of Presentations: 0.00

Non Peer-Reviewed Conference Proceeding publications (other than abstracts):

Number of Non Peer-Reviewed Conference Proceeding publications (other than abstracts): 0

Peer-Reviewed Conference Proceeding publications (other than abstracts):

Number of Peer-Reviewed Conference Proceeding publications (other than abstracts): 0

(d) Manuscripts

submitted:

S. A. Koepsell, M. A. Larson, C. A. Frey, S. H. Hinrichs, and M. A. Griep. Biochemistry (submitted)
Staphylococcus aureus Primase Is Less Stimulated by Its Helicase than Escherichia coli Primase

M. A. Larson, R. Bressani, K. Sayood, J. E. Corn, J. M. Berger, M. A. Griep, and S. H. Hinrichs. Nucleic Acids Research (submitted)
Aquifex aeolicus primase initiation specificity is distinct from Escherichia coli and Staphylococcus aureus

K.A. Bryant, S. H. Hinrichs and P. D. Fey.
Journal of Microbiology (submitted)
Transcriptional analysis of the macromolecular synthesis operon in Staphylococcus epidermidis.

Number of Manuscripts: 3.00

Number of Inventions:

Graduate Students

NAME	PERCENT_SUPPORTED
Rafael Bressani	1.00
Kendall Bryant	1.00
Chris Frey	1.00
FTE Equivalent:	**3.00**
Total Number:	**3**

Names of Post Doctorates

NAME	PERCENT_SUPPORTED
Scott Koepsell	1.00
FTE Equivalent:	**1.00**
Total Number:	**1**

Names of Faculty Supported

NAME	PERCENT_SUPPORTED	National Academy Member
Marilynn Larson	1.00	No
Steven H. Hinrichs	0.17	No
Mark Griep	0.25	No
FTE Equivalent:	**1.42**	
Total Number:	**3**	

Names of Under Graduate students supported

NAME	PERCENT_SUPPORTED
FTE Equivalent:	
Total Number:	

Student Metrics

This section only applies to graduating undergraduates supported by this agreement in this reporting period

The number of undergraduates funded by this agreement who graduated during this period:	0.00
The number of undergraduates funded by this agreement who graduated during this period with a degree in science, mathematics, engineering, or technology fields:.....	0.00
The number of undergraduates funded by your agreement who graduated during this period and will continue to pursue a graduate or Ph.D. degree in science, mathematics, engineering, or technology fields:.....	0.00
Number of graduating undergraduates who achieved a 3.5 GPA to 4.0 (4.0 max scale):	0.00
Number of graduating undergraduates funded by a DoD funded Center of Excellence grant for Education, Research and Engineering:	0.00
The number of undergraduates funded by your agreement who graduated during this period and intend to work for the Department of Defense	0.00
The number of undergraduates funded by your agreement who graduated during this period and will receive scholarships or fellowships for further studies in science, mathematics, engineering or technology fields:	0.00

Names of Personnel receiving masters degrees

NAME
Total Number:

Names of personnel receiving PHDs

NAME
Scott Koepsell M.D. Ph.D.
Total Number: 1

Names of other research staff

NAME	PERCENT_SUPPORTED	
Anna Hanway	1.00	No
FTE Equivalent:	**1.00**	
Total Number:	**1**	

Sub Contractors (DD882)

Inventions (DD882)

Appended Material

Table of contents and attachments.

1. Introduction

Antibiotic resistance in bacteria is a growing problem for military and civilian populations. A recent report from the CDC determined that methicillin resistant Staphylococcus (MRSA) caused more deaths in the United States in 2005 that occurred due to HIV infection. In addition, bacterial select agents may have been engineered to be resistant to many classes of currently available antibiotics. Therefore a great need exists for discovery of new targets for development of antibiotics.

We have identified a molecular target termed Dna G primase, that is a protein essential for bacterial DNA replication and meets the criteria for novel drug discovery. Biochemical and molecular studies were performed to characterize key interactions of primase with DNA and a second protein involved in the replication process termed helicase. The primase and helicase proteins for Staphylococcus aureus were cloned and expressed for proof of principle studies. The DNA binding specificities and the helicase stimulation response were characterized and shown to differ from E. coli, the only other bacteria studied prior to this work. This work is summarized in the attachment manuscript number 1.

2. Cloning and expression of new targets.

The goal of this project was to demonstrate that lessons learned in the prototype test system could be applied to other bacteria of special interest to the military including those that have been used as biological weapons. Subsequently, the primase and helicase from Yersinia pestis and Bacillus anthracis. To complete the analysis and clearly demonstrate

the broad spectrum and narrow spectrum application of our work we also selected other bacteria for study. Therefore Pseudomonas aerugenosa primase was cloned in our laboratories and the Geobacillus sterothermophilus and Aquifex aerolicus were cloned in laboratories of our collaborators and purified and tested in our laboratories. The goal of this work was to examine whether the results seen in S. aureus and E. coli were truly predictive of all bacteria. Therefore, we studied not only common pathogens, but also bacteria that grow in extreme environments, ie Aquifex aerolicus. Several problems had to be overcome, the most significant being the lack of solubility of primase when it is expressed at high concentration.

Results show that the biochemical interactions between primase and DNA are common among the Gram positive organisms studied to date and that the key determinants of this interaction are different from Gram negative organisms. Additional studies showed that the interactions between primase and helicase were unique and generally specific to the species under study. These findings were correlated with structural information regarding those proteins that have been crystallized. Results of these studies are described in published manuscript number 2 and submitted, but currently unpublished manuscripts number 1 and 2.

3. Computational screening.

Two different approaches were taken to identify inhibitory compounds including computational modeling and in silico screening of large chemical structure libraries, and two, chemical compound library screening. We identified one compound called myricetin that is a known inhibitor of helicases and kinases. We demonstrated that myricetin is an effective noncompetitive inhibitor of the ATPase activity of *E. coli* DnaB helicase (IC_{50} of 11 mM). This work helped position us to explore other compounds. The results of these studies are summarized in attached published manuscript 3. The computational screening identified 10 compounds which were subsequently evaluated. None of these compounds showed sufficient promise to be studied further and all efforts were directed to the second screening strategy.

4. Creation of a drug screening paradigm.

As our capability to produce and purify large quantities of primase improved, were were able to implement a more comprehensive strategy for identification of lead compounds and that was high throughput screening (HPT). A comprehensive drug screening paradigm was developed and 40,000 compounds tested. In the first screen, 800 compounds were identified that met the first level of activity, of which 12 were chosen in secondary screens and counter screens. In aggregate these studies have provided a comprehensive analysis of the biological properties of replicative primase and revealed the potential for an entirely new class of therapeutic agents with either broad spectrum or narrow spectrum coverage. The body of work is now ready for transfer to the next stage of development and partnering with a pharmaceutical or biotech company.

Attachment 4.1

Antimicrobial Discovery Project

Data analysis strategy and summary

Goal: Optimize the screening assay to detect a 50% reduction in activity in presence of inhibitor.

Experiment one. In the first experiment using our high throughput screening (HTS) assay on the primary screen selected TimTec library, we used 1800 nM Primase + 200 nM template with compound library concentrations of 20 nM. Under these conditions, it was expected that we would detect a 10% inhibition under the most favorable conditions. The screen was performed and it was found that the error in the assay was approximately 7%, and therefore it was unlikely that any of the potential hits were inhibitors with any confidence.

We explored two possibilities for dealing with this problem, either lower the enzyme and template to 20 nM, or use higher compound concentrations that are the same as the enzyme and template. A series of experiments were performed to test the feasibility of the first approach.

Second experiment: The fluorometric primer synthesis reaction were performed in duplicate using either 1/250 or 1/500 dilutions of PicoGreen; either 20, 500, or 1500 nM Primase; and either 20, 50, or 500 nM template.

Results:

The background fluorescence was the same regardless of PicoGreen dilution (data not shown). It was subtracted from all values to obtain the background-corrected fluorescence intensities.

Fo: The background-corrected initial fluorescence intensity Fo' is dependent on PicoGreen dilution. The average from about 17 runs (data not shown) established that Fo' was 14% lower when using 1/500 diluted PicoGreen. A low Fo is advantageous because our signal is determined by F/Fo.

Fmax/Fo: The maximum signal generated by each combination of primase and template is shown in the table below. In the presence of 20 nM Primase, the signal decreases as Template conc is increased above 20

Table 1: Scale Down Results

PicoGreen	[P]	[D]	Fmax/Fo	
1/250	20	20	2.24	
1/250	500	20	3.39	
1/250	1500	20	10.26	
1/250	20	50	1.08	
1/250	500	50	2.88	
1/250	1500	50	7.80	
1/250	20	200	0.95	
1/250	500	200	2.98	Ratio of
1/250	1500	200	7.36	500/250
1/500	20	20	1.54	0.69
1/500	500	20	3.35	0.99
1/500	1500	20	10.42	1.02
1/500	20	50	0.94	0.87
1/500	500	50	3.12	1.08
1/500	1500	50	7.70	0.99
1/500	20	200	0.76	0.80
1/500	500	200	3.30	1.11
1/500	1500	200	8.28	1.13

nM. This makes sense because fewer templates can be primed and the Fo increases due to so much free Template. In the presence of 500 or 1500 nM primase, the signal is constant or even decreases as the Template is increased to 200 nM.

PicoGreen dilution: Since all reactions were performed at two different dilutions of PicoGreen, the ratio of the two signals can be compared. The average of ratio of the 1/500 dilution to the 1/250 dilution is 1.00 ± 0.11 indicating that there is no difference in the magnitude of the Fmax/Fo despite the different dilutions. This means that the 1/500 should be used to save costs and to make use of the 14% lower Fo.

Z-factor: The utility of an assay for HTS is determined by its Z-factor. The Z-factor calculation determines the 95% confidence of the assay. If the Z-factor is between 0.5 and 1.0, then the ability to determine "hits" is considered excellent. The equation is $Z\text{-factor} = 1 - (3 \times (\sigma p + \sigma n))/(\mu p - \mu n)$, where σ is the standard deviation, μ is the average, p is the positive control signal, and n is the negative control. In the case of the "Scale Down Test", the standard deviation was approximately 0.07.

The 20 nM Primase and 20 nM Template data set indicates that Fmax/Fo is 2.24 for the 1/250 PicoGreen dilution. Since our negative control generates an Fo/Fo of 1.00, all of the numbers can be inserted into the Z-factor equation to find that it is 0.66.

Experiment 3. Determine the optimal concentration of DMSO with the goal of increasing the signal to greater than 2. Previously, we used 2% DMSO in the HTS assay. Therefore, 2% (previous HTS condition), 10%, 20%, & 40% DMSO was tested.
Results: results showed that 20% increased the signal the most, whereas, 40% DMSO inhibited DnaG.

Experiment 4. Optimization of enzyme and template concentrations. Triplicate test reactions were performed w/ 20% DMSO w/o & w/ either 2.5% & 5% PEG & [SaP]= [template] in either a 20 uL or 40 uL rxn. More specifically, 200 nM SaP w/ 200 nM template, 100 nM SaP w/ 100 nM template, 50 nM SaP w/ 50 nM template, & 25 nM SaP w/ 25 nM template was evaluated.

Results. Results demonstrated that the optimal concentration of SaP was 200 nM. Further, PEG did not increase the signal in the presence of DMSO. The % error was the same for the 20 uL & 40 uL rxns. So we now know that we can use 200 nM SaP, 200 nM template in a 20 uL rxn that contains 20% DMSO with a 1:250 PicoGreen dilution & probably even a 1:500 PicoGreen dilution (see Experiment 3 description above for PicoGreen dilutions).

Conclusion: The assay has been optimized to identify hits using 200 nM Primase and Template with 20% DMSO.

5. Demonstration of genus specific modularity of primase in bacteria

Based on the work described above, we belived that primase initiation specificity in all Firmicutes and Gamma-proteobacteria would differ, but that the DnaG recognition sequences would be shared by members within these bacterial classes. To examine the mechanistic details of the modular functions of bacterial primase we have swapped the Zinc-binding domain (ZBD), RNA polymerase domain (RPD), and C-terminal domain (CTD) from the Gram-positive Firmicute *Staphylococcus aureus* primase and the Gram-negative Gamma-proteobacteria *Escherichia coli* primase. In this work we confirmed the modularity of primase's three domains, as well as clarified their function. More specifically, both the ZBD and the RPD of primase were shown to contribute to primer synthesis in that the ZBD influenced template specificity and the RPD regulated processivity.

Experiments were performed to evaluate primase-helicase cross stimulation between the chimeric primases, as well as members of these two different bacterial classes. We determined that the CTD of primase interacts with helicase, but the relative ability of Gram-positive Firmicute and Gram-negative Gamma-proteobacteria helicases to stimulate primase within the same bacterial class is limited in that only closely related

microbes can cross-stimulate. Collectively, these results provide clues to the domain(s) involved in primase-helicase and protein-nucleic acid interactions, as well as features shared or unique to these two divergent bacterial classes of primases.

This work is summarized in the material presented below. This will be the basis of a manuscript that has not been submitted at the time of this report.

INTRODUCTION

We hypothesized that Gram-positive Firmicute primases have trinucleotide initiation specificities that are similar to each other, but that differ from those of Gram-negative Gamma-proteobacterial primases. In addition, we propose that template recognition is associated with specific residues in the N-terminal Zinc Binding Domain (ZBD), but influenced by the processivity of the RNA Polymerase Domain (RPD). We also hypothesis that the C-terminal Domain (CTD) of primase interacts directly with the hexameric helicase, but that an increase in primer synthesis only occurs when both of these replication proteins are from the same or closely related bacteria.

To date primase initiation specificity for two Firmicutes and three Gamma-proteobacteria, as well a member of the bacterial class Aquificae, has been determined. We have determined that *Bacillus anthracis* share initiation specificity with other Firmicutes.

RESULTS

Initiation Specificity of Firmicutes, Gamma-proteobacteria, and Aquificae bacterial DnaG primases

Table 1. Bacterial Genome Content, Primase Sequence Homology, and Primase Initiation Specificity.

Primer synthesis assays with the *B. anthracis* DnaG revealed that CTA was the preferred initiation trinucleotide and that TTA was also recognized, but to a much reduced level, confirming that primases from Firmicutes have the same initiation specificity (Table 1). Therefore, Firmicutes and Gamma-proteobacteria share primase initiation trinucleotides with other members within that bacterial class and that these DnaG recognition trinucleotides differ from a member of the group Aquificae.

Functional role of each domain in bacterial primase

Figure 1. *De novo* primer synthesis by the CTD swapped primases. Comparison of primer synthesis by wild-type DnaG from *S. aureus* and *E. coli* to CTD swapped primases using ssDNA templates that contain **(A)** the *S. aureus* primase recognition trinucleotides CTA or TTA or **(B)** the *E. coli* primase initiation sequence CTC.

Results showed that the CTD from *E. coli* DnaG did not substantially alter priming specificity by the *S. aureus* ZBD and RPD with the Firmicute primase recognition sequences CTA or TTA (Figure 1A). Similar to wild-type *E. coli* primase, the chimeric primase containing the ZBD and RPD from *E. coli* primase with the CTD from *S. aureus* primase did not produce any primers with the Firmicute TTA initiation sequence and both primases had only minimal activity with the CTA template.

Data showed that the CTD of *E. coli* DnaG is not required for primer production on the preferred *E. coli* primase initiation sequence CTC (Figure 1B). Moreover, neither the absence of the *E. coli* primase CTD nor the presence of the *S. aureus* CTD altered the length or amount of primers synthesized by the chimeric primase containing the *E. coli* primase ZBD and RPD with the *S. aureus* primase CTD. The wild-type *S. aureus* primase and the chimeric primase containing the *S. aureus* primase ZBD and RPD with the *E. coli* primase CTD only had minimal activity with the CTC template.

Collectively, these results demonstrate that the CTD of DnaG does not substantially influence class-specific template recognition or primer synthesis in the absence of helicase.

Figure 2. Primer synthesis on the CTA and CTC templates by the chimeric protein containing the ZBD of *S. aureus* primase and the RPD and CTD of *E. coli* primase.

Priming on the Firmicute recognition sequence CTA was retained by the ZBD swapped chimera containing the *S. aureus* primase ZBD, demonstrating that the ZBD does indeed have a substantial role in template recognition. However, the amount of full-length primers was reduced without the presence of the cognate *S. aureus* primase RPD.

In addition, the chimeric primase containing the ZBD of *S. aureus* primase recognized the initiation trinucleotide CTC preferred by wild-type *E. coli* primase. These results showed that the presence of the *E. coli* primase RPD contributed to the high abundance of primers produced which was approximately 2-fold higher than the amount of primers synthesized by wild-type *E. coli* primase with this template (Figure 1). These data suggested that the high processivity of the *E. coli* primase RPD releases template specificity in this ZBD swapped chimeric primase and that the *E. coli* primase ZBD may also have a regulatory role that negatively affects primer synthesis by wild-type *E. coli* primase.

Comparison of the different RNA polymer lengths produced with templates containing the preferred Firmicute initiation trinucleotide CTA by the chimera containing the *E. coli* primase ZBD and RPD and the CTD of *S. aureus* primase (Figure 1) with that of the chimera containing the ZBD of *S. aureus* primase and the RPD and CTD of *E. coli* primase (Figure 2) were similar, but the amount of primers produced by the later DnaG chimera were substantially higher. These data further demonstrated the high processivity of the *E. coli* primase RPD when present, but that the ZBD is predominately responsible for template specificity.

Unfortunately, the activity of the chimera containing the ZBD of *E. coli* primase and the RPD and CTD of *S. aureus* primase was minimal and no trinucleotide specificity was observed with either the CTA or CTC templates (data not shown).

Collectively, these results showed that the ZBD swapped primase exhibited hybrid activity without the presence of the cognate RPD, but that template specificity is predominately determined by the ZBD and that processivity is controlled by the RPD.

Figure 3. Residues in the ZBD of DnaG that contribute to template recognition. **(A)** Multiple sequence alignment of bacterial primase ZBD from selected Firmicutes, Gamma-proteobacteria, and Aquificae. **(B)** Primer synthesis on the various trinucleotide templates by modified DnaG proteins with single and double mutations in the ZBD.

Figure 4. Primer synthesis by *S. aureus* and *E. coli* primases without their cognate CTD either in the absence or presence of their respective helicase.

The ZBD and RPD of the primases from *S. aureus* or *E. coli* primase were sufficient for *de novo* primer synthesis. In fact the apparent activity of the truncated DnaG without the CTD was higher than the full-length primase, suggesting that the CTD negatively regulates the activity of the native bacterial primases. However, the activity of these truncated primases was inhibited by the presence of their respective helicase, demonstrating that helicase stimulated primer synthesis requires the CTD of primase.

Figure 5. Helicase stimulation of the CTD and ZBD swapped chimeric primases. **(A)** *S. aureus* helicase stimulation of the chimeric primase containing the *E. coli* primase ZBD and RPD and the *S. aureus* primase CTD. **(B)** *E. coli* helicase stimulation of the chimeric primase containing the *S. aureus* primase ZBD and RPD and the *E. coli* primase CTD and the chimeric primase containing the *S. aureus* primase ZBD and the *E. coli* primase RPD and CTD.

Unexpectedly, the chimeric primase containing the *E. coli* primase ZBD and RPD with the *S. aureus* primase CTD was stimulated by *S. aureus* helicase using the Firmicute-specific CTA template (Figure 5A), but not with the CTC template (data not shown). These results suggested that *S. aureus* helicase does interact with the *S. aureus* CTD, but that the specificity changes without the cognate ZBD and RPD.

Again the activity of the chimera containing the ZBD of *E. coli* primase and the RPD and CTD of *S. aureus* primase was minimal, regardless of trinucleotide-specific template used, and was not stimulated by the presence of *S. aureus* helicase (data not shown).

The presence of *E. coli* helicase influenced primer synthesis by the chimeric primase containing the *S. aureus* primase ZBD and RPD and the *E. coli* primase CTD such that the length of the primers were reduced, similar to the stimulation of wild-type *E. coli* primase by *E. coli* helicase (Figure 5B). However, the amount of primers produced by the chimeric primase was substantially reduced. These results show that *E. coli* helicase does interact with the *E. coli* primase CTD. However, the presence of the cognate CTD to the helicase used for stimulation is not sufficient for optimum stimulation, suggesting that the interaction between the ZBD and RPD of DnaG is altered.

Although both the RPD and CTD of *E. coli* primase were present in the chimeric primase containing the *S. aureus* primase ZBD, *E. coli* helicase inhibited primer synthesis

(Figure 5B). Overall, these data suggested that helicase stimulation modulated primer synthesis by a conformational change that alters the interaction between all three primase domains, especially if the ZBD and RPD of primase are not from the same bacterium. These results further support the notion that the primase-helicase interaction *in vivo* has evolved such that these essential proteins regulate each others activity via modulation of the various domains.

Figure 6. *In vivo* rescue of *E. coli dnaG* mutant with wild-type *E. coli* DnaG and chimeric primases that contain the CTD from *E. coli* DnaG.

Species specificity of primase-helicase interactions

Figure 7. Cross-stimulation of Firmicute and Gamma-proteobacterial primases and helicases. **(A)** *S. aureus* helicase stimulation of primases from *B. anthracis* and *G. stearothermophilus* and vice versa. **(B)** *E. coli* helicase stimulation of primases from *Y. pestis* and *P. aeruginosa* and vice versa.

G. stearothermophilus helicase inhibited *S. aureus* primase activity possibly due to inherent differences between mesophilic versus thermophilic replication enzymes (Figure 7A).

E. coli helicase stimulated *Y. pestis* primase and *Y. pestis* helicase stimulated *E. coli* primase. However, the helicases from *E. coli* and *Y. pestis* did not stimulate *P. aeruginosa* primase, nor did *P. aeruginosa* helicase stimulate the primases from *E. coli* and *Y. pestis* (Figure 7B). Collectively, these results demonstrated that the replicative helicase must be from closely related bacteria in order to functionally interact with DnaG and stimulate primer synthesis.

Structural differences in Firmicute and Gamma-proteobacterial DnaG CTDs

Figure 8. Model of primase-helicase complex at DNA replication fork.

Confirmed modularity of DnaG primase's three domains: the ZBD, the RPD and the CTD, as well as clarified the functional role of these domains.

Domain swapping of primase from *S. aureus* and *E. coli* revealed that the CTD swapped chimeras exhibited activity that corresponded to the chimeric primase ZBD and RPD and that primer synthesis was similar to that of the wild-type DnaG in the absence of helicase. Therefore, the presence of a CTD from a primase that is from a different bacterial class, has a minimal role in primer synthesis activity by the ZBD and RPD in the absence of helicase. In contrast, the ZBD swapped primases displayed hybrid activity, suggesting that any modulation of the linker region between the ZBD and RPD will alter primer production. Overall, these results demonstrated that the ZBD influences trinucleotide specificity and that the RPD controls processivity.

Demonstrated that the ZBD and RPD of bacterial primases are sufficient for *de novo* primer synthesis and therefore, confirmed that the CTD is not required for primer synthesis in the absence of helicase. In addition, these truncated primases have higher activity than the corresponding full-length DnaG in the absence of helicase and that in the presence of helicase, primase activity by the ZBD and RPD was inhibited, suggesting an autoregulatory role for the CTD.

Species specificity of primase-helicase interactions

CTD domain swapping of primase from *S. aureus* and *E. coli* revealed that the presence of the CTD that corresponds to the helicase was not sufficient for stimulated primer synthesis and that the interaction between all three primase domains was critical for helicase stimulated primer synthesis.

Cross-stimulation between primase and helicase was restricted to only closely related members of the same bacterial class.

Structural differences in Firmicute and Gamma-proteobacterial DnaG CTDs

A model was proposed of the primase-helicase complex that explains the productive interaction of these essential proteins at the replication fork that results in stimulated primer synthesis and that is species specific.

FIGURES and FIGURE LEGENDS

Table 1. Bacterial Genome Content, Primase Sequence Homology, and Primase Initiation Specificity.

Gram-positive Firmicutes

Microbe	G/C Content[a]	Overall/ZBD %ID (% Similarity)[b]	Trinucleotide Initiation Specificity
S. aureus (N315)	33%	100 (100)/100 (100)	CTA>TTA
B. anthracis (Ames)	35%	37 (51)/53 (64)	CTA>TTA[d]
G. stearothermophilus	NA[e]	36 (47)/53 (61)	CTA>TTA[f]

Gram-negative Gamma-proteobacteria

Microbe	G/C Content[a]	Overall/ZBD %ID (% Similarity)[b]	Trinucleotide Initiation Specificity
E. coli (K12)	51%	100 (100)/100 (100)	CTC>CTG
Y. pestis (CO92)	48%	77 (82)/90 (96)	CTG>CTA
P. aeruginosa (PA01)	67%	56 (67)/63 (74)	CTG>CTA

Gram-negative Aquificae

Microbe	G/C Content[a]	Overall/ZBD %ID (% Similarity)[c]	Trinucleotide Initiation Specificity
A. aeolicus	43%	34(47)/48 (55) & 36 (48)/41 (49)	CGC>CCG

[a]Percent G/C content in the bacterial chromosome.
[b]Primase sequence identity and similarity are relative to *S. aureus* DnaG for the Firmicutes and relative to *E. coli* DnaG for the Gamma-proteobacteria.
[c]Primase sequence identity and similarity are relative to *S. aureus* DnaG and *E. coli* DnaG, respectively.
[d]Primase initiation specificity determined in this study.
[e]Microbial genome sequencing project not incomplete and in-progress.
[f]Data derived from Twirlway and Soultanas (2006) and confirmed by our laboratory.

Figure 1. *De novo* primer synthesis by the CTD swapped primases. Comparison of primer synthesis by wild-type DnaG from *S. aureus* and *E. coli* to CTD swapped primases using ssDNA templates that contain **(A)** the *S. aureus* primase recognition trinucleotides CTA or TTA or **(B)** the *E. coli* primase initiation sequence CTC.

A

Legend
10 = SaP(Z+R)/EcP(C)
13 = EcP(Z+R)/SaP(C)

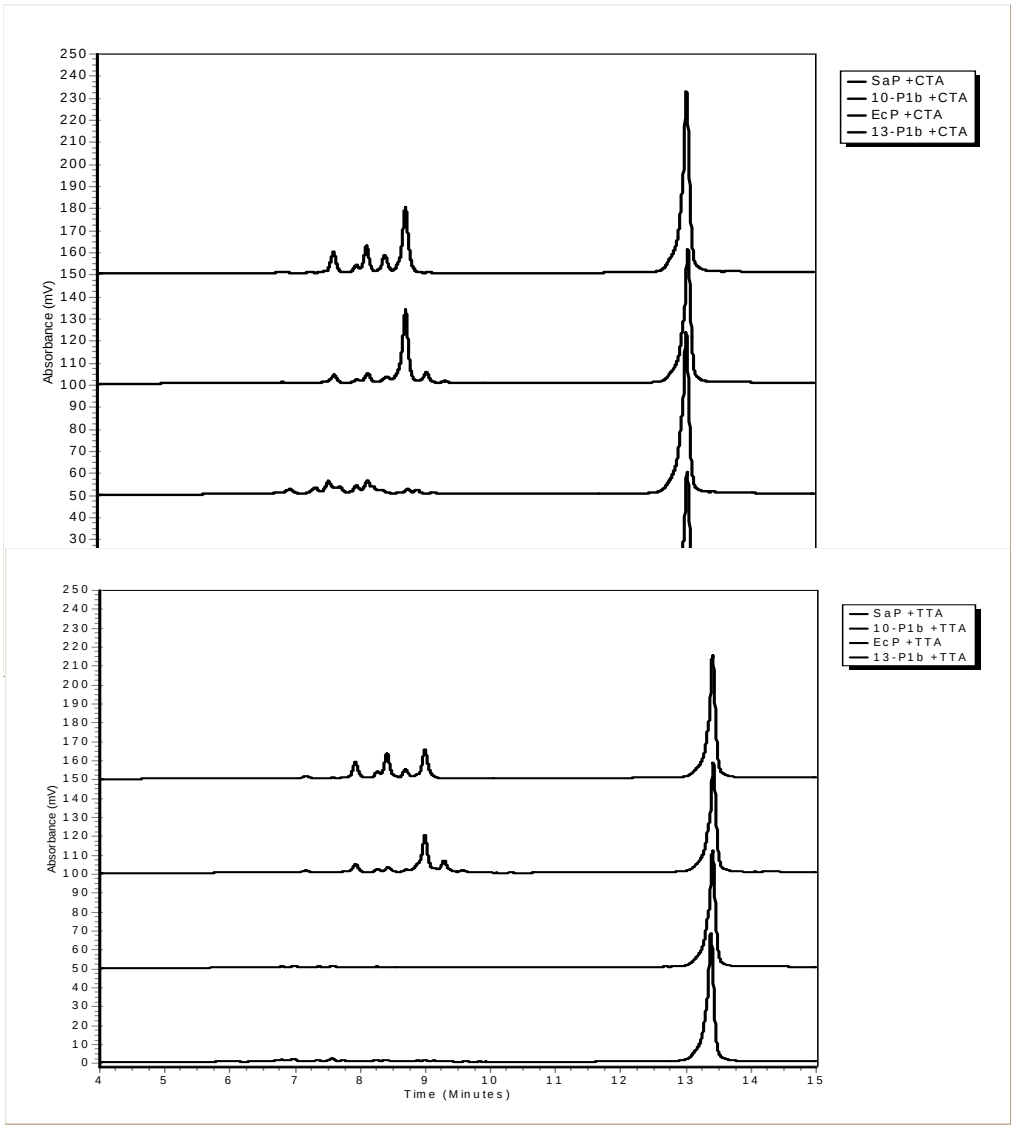

B

Legend
10 = SaP(Z+R)/EcP(C)
13 = EcP(Z+R)/SaP(C)

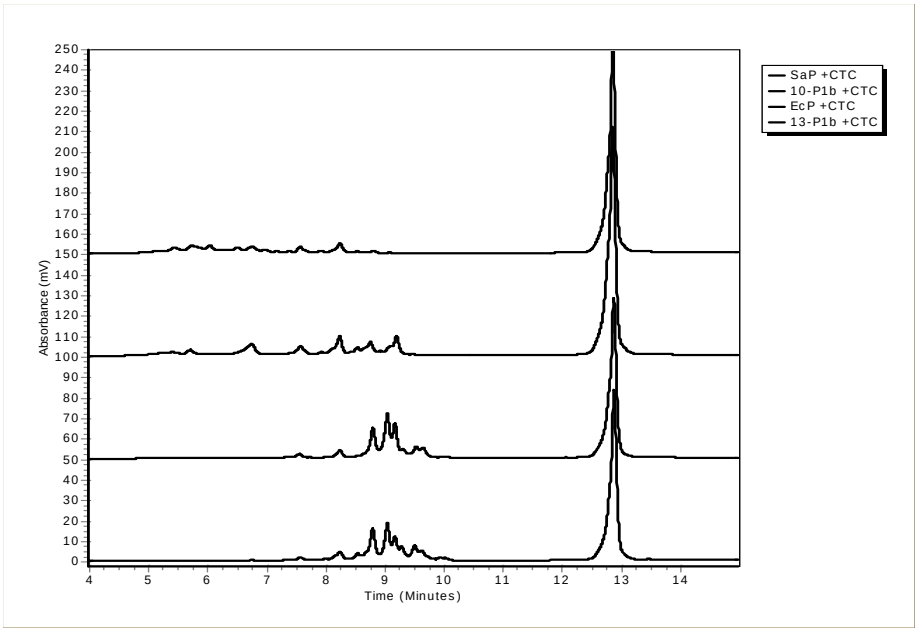

Figure 2. Primer synthesis on the CTA and CTC templates by the chimeric protein containing the ZBD of *S. aureus* primase and the RPD and CTD of *E. coli* primase.

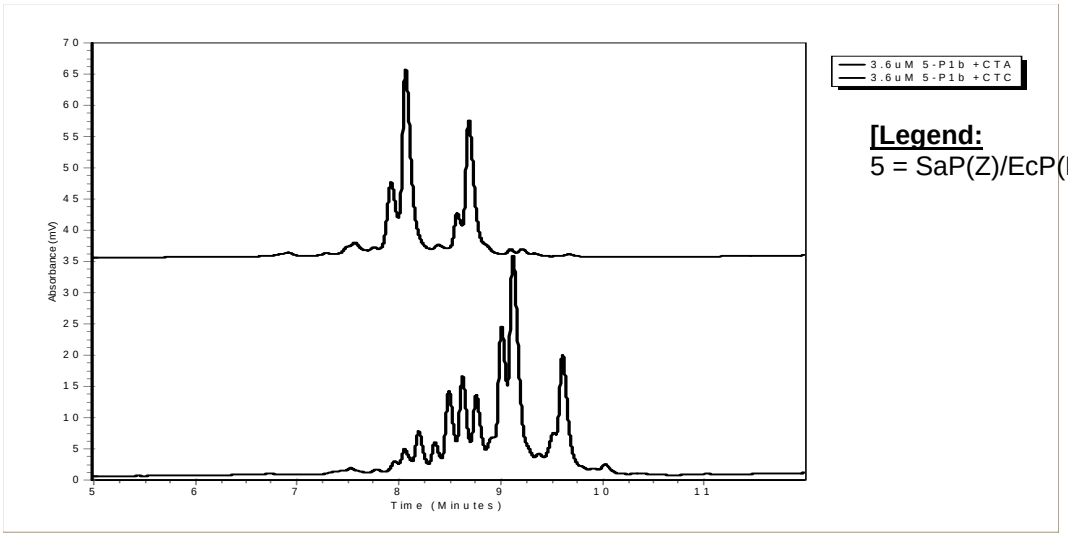

Figure 3. Residues in the ZBD of DnaG that contribute to template recognition. **(A)** Multiple sequence alignment of bacterial primase ZBD from selected Firmicutes, Gamma-proteobacteria, and Aquificae. **(B)** Primer synthesis on the various trinucleotide templates by modified DnaG proteins with single and double mutations in the ZBD.

A

B

Figure 4. Primer synthesis by *S. aureus* and *E. coli* primases without their cognate CTD either in the absence or presence of their respective helicase.

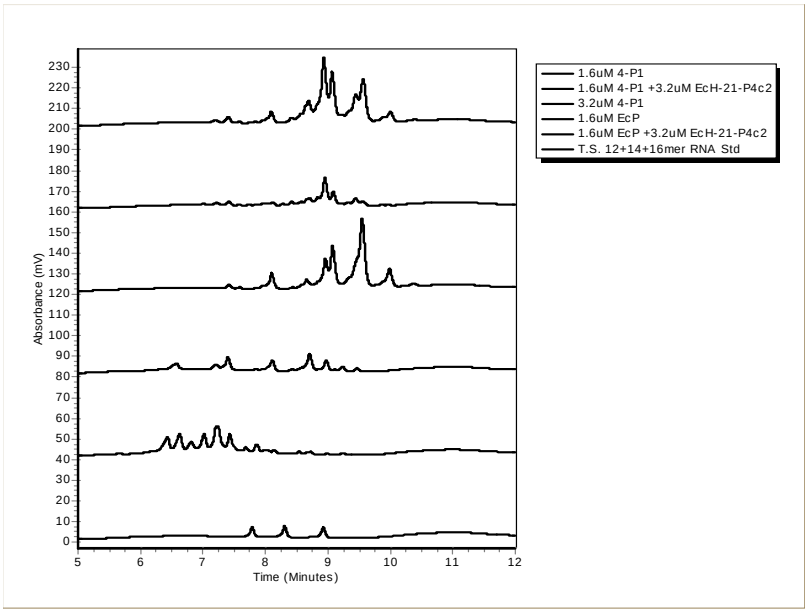

Legend:
4 = EcP(Z+R)
2 = SaP (Z+R)

Figure 5. Helicase stimulation of the CTD and ZBD swapped chimeric primases. **(A)** *S. aureus* helicase stimulation of the chimeric primase containing the *E. coli* primase ZBD and RPD and the *S. aureus* primase CTD. **(B)** *E. coli* helicase stimulation of the chimeric primase containing the *S. aureus* primase ZBD and RPD and the *E. coli* primase CTD and the chimeric primase containing the *S. aureus* primase ZBD and the *E. coli* primase RPD and CTD.

A

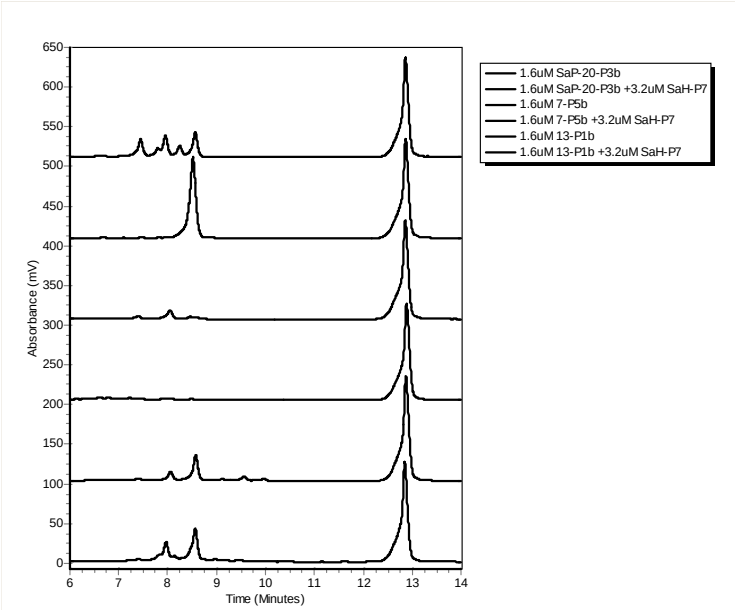

Legend
Clone13 = EcP(Z+R)/SaP(C) -/+ SaH
Clone 7 = EcP(Z)/SaP(R+C) -/+ SaH

B

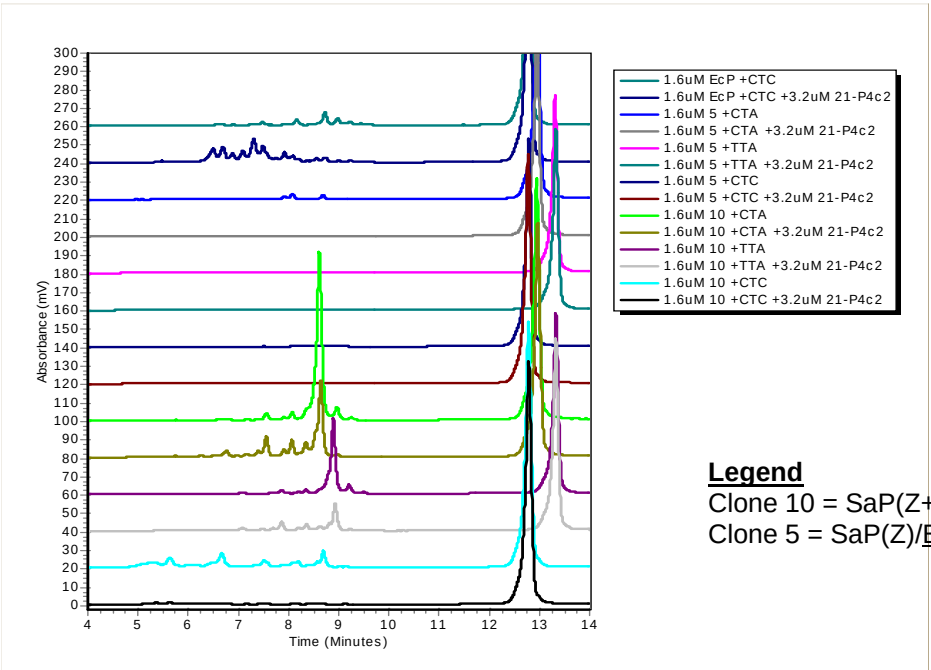

Legend
Clone 10 = SaP(Z+R)/EcP(C) -/+ EcH
Clone 5 = SaP(Z)/EcP(R+C) -/+ EcH

Figure 6. *In vivo* rescue of *E. coli dnaG* mutant with wild-type *E. coli* DnaG and chimeric primases that contain the CTD from *E. coli* DnaG.

Legend:

Wild-type EcP w/ & w/o N-terminal His6 tag (+ control): Expect high growth at nonpermissive temperature

Clone 13 = EcP(Z+R)/SaP(C) (- control): Expect no growth at nonpermissive temperature

Clone 10 = SaP(Z+R)/EcP(C): Expect slight growth at nonpermissive temperature

Clone 5 = SaP(Z)/EcP(R+C): Expect very slight growth at nonpermissive temperature

II.) Species specificity of primase-helicase interactions.

Figure 7. Cross-stimulation of Firmicute and Gamma-proteobacterial primases and helicases. **(A)** *S. aureus* helicase stimulation of primases from *B. anthracis* and *G. stearothermophilus* and vice versa. **(B)** *E. coli* helicase stimulation of primases from *Y. pestis* and *P. aeruginosa* and vice versa.

A

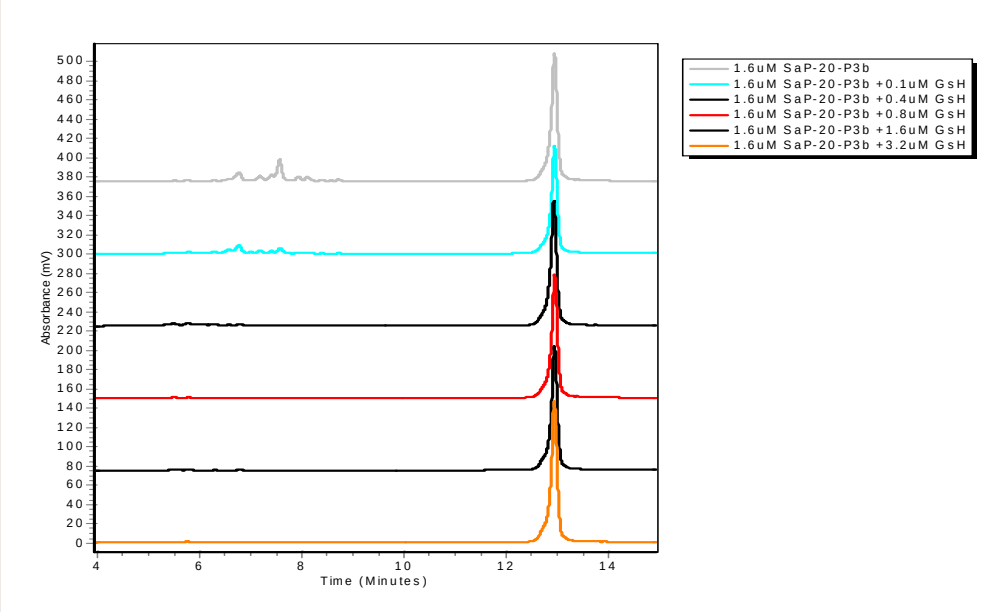

G. stearothermophilus helicase inhibited *S. aureus* primase activity possibly due to inherent differences between mesophilic versus thermophilic replication enzymes (Figure 7A).

B

E. coli helicase stimulated *Y. pestis* primase and *Y. pestis* helicase stimulated *E. coli* primase. However, the helicases from *E. coli* and *Y. pestis* did not stimulate *P. aeruginosa* primase, nor did *P. aeruginosa* helicase stimulate the primases from *E. coli* and *Y. pestis* (Figure 7B). Collectively, these results demonstrated that the replicative helicase must be from closely related bacteria in order to functionally interact with DnaG and stimulate primer synthesis.

IV.) Structural differences in Firmicute and Gamma-proteobacterial DnaG CTDs.

Figure 8. Model of primase-helicase complex at DNA replication fork.

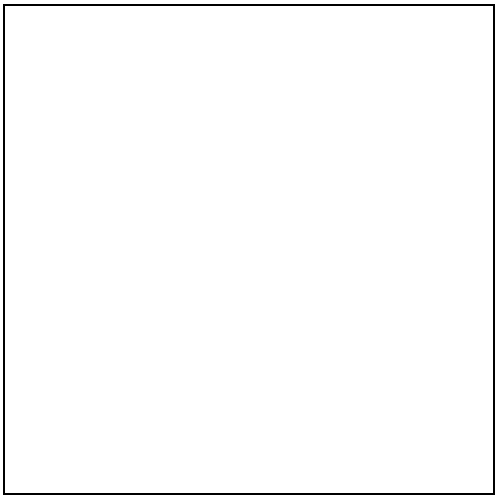

DISCUSSION

Data obtained to date by our studies strongly suggest that primases from both Firmicutes and Gamma-proteobacteria preferentially initiate *de novo* primer synthesis on a CTN trinucleotide in the template and subsequently produce a primer that begins with 5'-AG-3', differing from *Aquifex aeolicus* initial ribonucleotides 5'-CG-3'. We propose that the primases from Gram-positive Firmicutes initiated primer synthesis on the trinucleotide CTA and probably evolved to use trinucleotide TTA due to their AT-rich genome, supporting a relationship between primer synthesis initiation and genome content. Gram-negative bacterial primases that presumably evolved from Gram-positive Firmicutes evolved to preferentially initiate primer synthesis on DNA templates that contain CT(G/C) since their genomes contain a relatively higher G+C content. In contrast, *A. aeolicus* most likely evolved from Firmicutes and adapted to an environment with high temperatures by using initiation trinucleotides that are comprised of all guanines and cytosines (CGC>CCG), enhancing the stability of the DNA-RNA complex during the rate limiting primer synthesis step of dinucleotide formation.

5-26-07ML

Attachment 5
Primase Screening Strategy

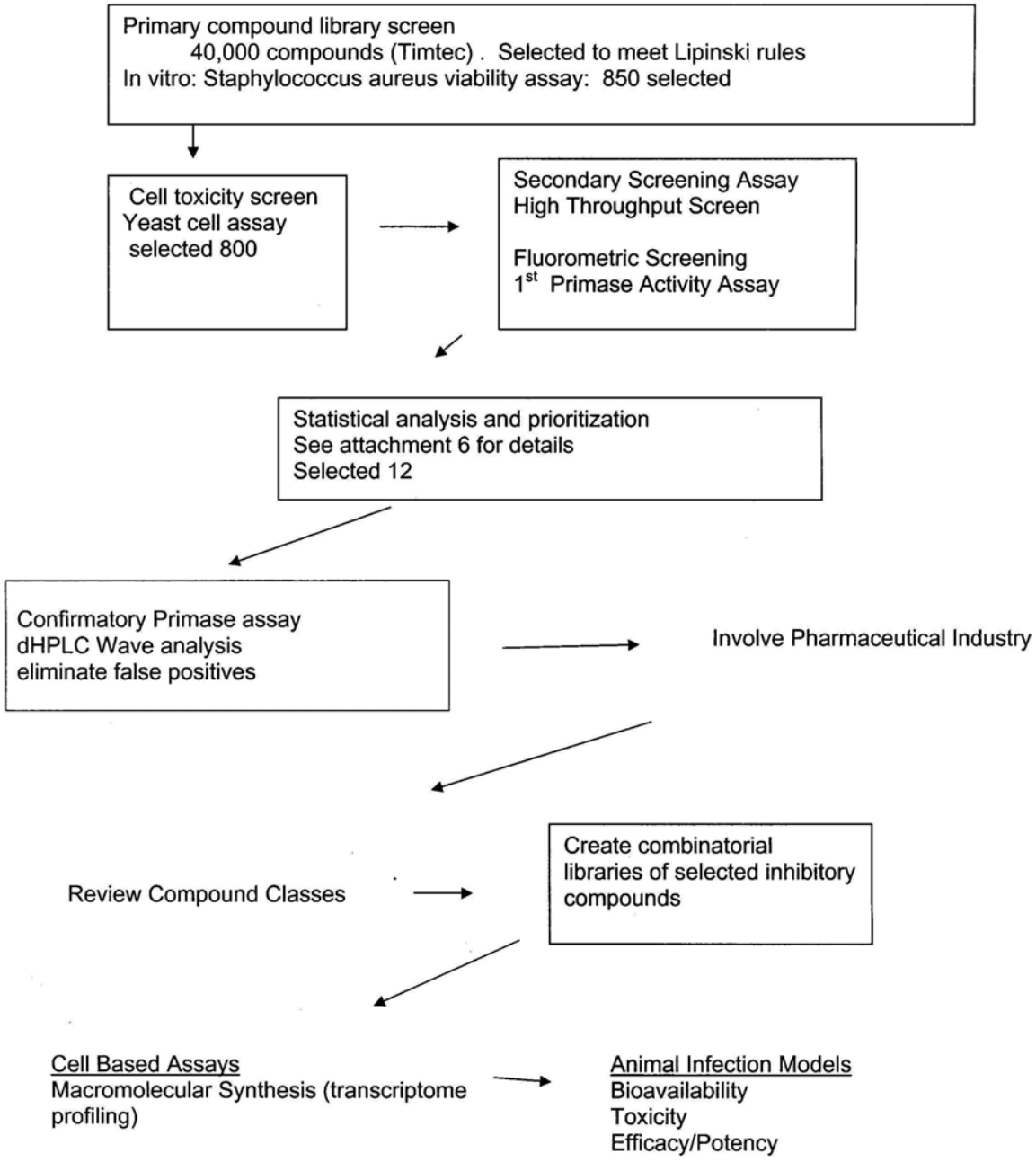

JOURNAL OF BACTERIOLOGY, July 2006, p. 4673–4680 Vol. 188, No. 13
0021-9193/06/$08.00+0 doi:10.1128/JB.00316-06

Staphylococcus aureus Helicase but Not *Escherichia coli* Helicase Stimulates *S. aureus* Primase Activity and Maintains Initiation Specificity†

Scott A. Koepsell,[1,2] Marilynn A. Larson,[1,2] Mark A. Griep,[2,3]* and Steven H. Hinrichs[1,2]

Department of Microbiology and Pathology, University of Nebraska Medical Center, Omaha, Nebraska 68198-6495[1]; University of Nebraska Center for Biosecurity, Omaha, Nebraska 68198-6495[2]; and Department of Chemistry, University of Nebraska—Lincoln, Lincoln, Nebraska 68588-0304[3]

Received 3 March 2006/Accepted 17 April 2006

Bacterial primases are essential for DNA replication due to their role in polymerizing the formation of short RNA primers repeatedly on the lagging-strand template and at least once on the leading-strand template. The ability of recombinant *Staphylococcus aureus* DnaG primase to utilize different single-stranded DNA templates was tested using oligonucleotides of the sequence 5′-CAGA $(CA)_5$ XYZ $(CA)_3$-3′, where XYZ represented the variable trinucleotide. These experiments demonstrated that *S. aureus* primase synthesized RNA primers predominately on templates containing 5′-d(CTA)-3′ or TTA and to a much lesser degree on GTA-containing templates, in contrast to results seen with the *Escherichia coli* DnaG primase recognition sequence 5′-d(CTG)-3′. Primer synthesis was initiated complementarily to the middle nucleotide of the recognition sequence, while the third nucleotide, an adenosine, was required to support primer synthesis but was not copied into the RNA primer. The replicative helicases from both *S. aureus* and *E. coli* were tested for their ability to stimulate either *S. aureus* or *E. coli* primase. Results showed that each bacterial helicase could only stimulate the cognate bacterial primase. In addition, *S. aureus* helicase stimulated the production of full-length primers, whereas *E. coli* helicase increased the synthesis of only short RNA polymers. These studies identified important differences between *E. coli* and *S. aureus* related to DNA replication and suggest that each bacterial primase and helicase may have adapted unique properties optimized for replication.

Bacterial genomes contain multiple RNA polymerase enzymes, of which *dnaG* encodes the sole primase involved in replication. As shown by temperature-dependent mutation studies, DnaG primase is essential for DNA replication and bacterial survival, leading to its identification as a possible target for antibiotic development (9, 14). However, little is known about the differences in primase structure and function among eubacteria, since only the primases from *Escherichia coli* and *Geobacillus* (formerly *Bacillus*) *stearothermophilus* have been studied in detail (22, 23).

The RNA polymer synthesized by primase is essential for providing a free 3′ hydroxyl group from which DNA polymerase can elongate. DNA polymerase cannot synthesize a nucleotide polymer de novo. Primase functions at least once during leading-strand synthesis and multiple times during lagging-strand synthesis, where the RNA primers are extended by DNA polymerase to form Okazaki fragments that are processed and ligated together into progeny genomes.

Replicative primases from viruses and phages have been shown to require a specific recognition sequence in order to synthesize an RNA polymer de novo. However, several studies suggested that the preferred primase binding sequences may differ among different bacteria genera (2, 6). Bacterial primases show approximately 39% sequence homology over the three major domains: the zinc-binding domain, the RNA polymerase domain, and the carboxy-terminal domain. The sequencing of many different bacteria has allowed comparison of primase regions, and although the proposed DNA-binding domain is conserved overall, a number of residues potentially involved in molecular interactions are variable among different species. We noted that certain residues are divergent within the zinc-binding domain that may interact with single-stranded DNA (ssDNA), as suggested by X-ray crystallography (16). Therefore, we hypothesized that these amino acid differences might affect primase initiation specificity.

The domain of primase with greatest variability in amino acid composition and the lowest homology among species is the carboxy-terminal domain (7). Biochemical and structural studies have demonstrated that the carboxy-terminal domain of *E. coli* DnaG is an important mediator of the primase-helicase interaction (15). *E. coli* DnaB helicase has been shown to modulate DnaG primase by stimulating the kinetics of primer synthesis, shortening the length of the primers, and releasing the initiation specificity of primase such that almost any ssDNA supports primer synthesis (2, 11).

The potential for a correlation between primase DNA binding specificity and genome content was first suggested by Blattner et al., who demonstrated that the most overrepresented 8-bp sequences in the *E. coli* genome contain the trinucleotide binding site for DnaG primase and are preferentially located on the strand of DNA that serves as the lagging-strand template (3). Bioinformatic analysis has since demonstrated the presence of overrepresented sequences that are biased toward

* Corresponding author. Mailing address: Department of Chemistry, University of Nebraska—Lincoln, Hamilton Hall 614, Lincoln, NE 68588-0304. Phone: (402) 472-3429. Fax: (402) 472-9402. E-mail: mgriep1@unl.edu.

† Supplemental material for this article may be found at http://jb.asm.org/.

one of the replicating strands, termed skewed oligomers, in every eubacterial genome analyzed (19). The conservation of the skewed oligomers throughout many unrelated genomes suggests that they contribute to the overall fitness of eubacteria. However, it is unknown whether the overrepresented sequences correlate with the DNA binding site for DnaG primase in other eubacteria.

Given its substantial increase in antibiotic resistance, *S. aureus* is of significant biological and medical importance. In contrast with the gram-negative bacterium *E. coli*, whose genome has a GC content of 50.8%, the gram-positive bacterium *S. aureus* has an AT-rich genome with only 32.8% GC content. Therefore, *S. aureus* was chosen for this investigation to determine whether primase binding specificity and activity are restricted at the genus level as well as to assess whether a correlation exists with genome content. We have cloned, expressed, and purified both *S. aureus* DnaG primase and DnaC helicase for biochemical analyses. The ability of *S. aureus* primase to utilize different ssDNA templates was examined using denaturing high-pressure liquid chromatography (HPLC) to analyze primer composition and quantity. Here we report that *S. aureus* DnaG primase utilizes three initiation sequences that are distinct from that of *E. coli*, the best-characterized bacterial primase, but similar to that of another gram-positive bacteria, *G. stearothermophilus* (23). *S. aureus* DnaC helicase was found to stimulate a substantial increase in *S. aureus* DnaG primase activity that resulted in the synthesis of RNA primers that were predominately full length. In addition, experiments were performed assessing the ability of replicative helicases from both *S. aureus* and *E. coli* to stimulate either *S. aureus* or *E. coli* primase. These studies demonstrated that the helicase of one bacterial species could not stimulate the primase of the other bacterial species.

MATERIALS AND METHODS

Generation of the ssDNA templates. Deoxyribonucleotides of the sequence 5′-CAGA $(CA)_5XYZ(CA)_3$-3′, where XYZ was AAA, AAG, AAT, ATA, ATC, ATT, CAG, CAT, CGA, CTA, CTC, CTG, CTT, GAA, GTA, TAA, TAG, TAT, TTA, TTC, TTG, or TTT, were generated by the University of Nebraska Core Facility or Integrated DNA Technologies (Coralville, IA). The oligonucleotides contained a 3′ C3 spacer that is required to prevent primase from elongating from a stabilized 3′ hairpin (2, 12). Purification of the ssDNA templates was performed using urea-polyacrylamide gel electrophoresis, UV shadowing, and elution of the oligonucleotide into Tris-EDTA buffer. Quantitation was performed using spectrophotometry at 260 nm with the respective extinction coefficients.

Construction of plasmid for the expression of recombinant *S. aureus* DnaG. The open reading frame of *dnaG* from *S. aureus* sp. strain N315 was amplified by PCR using primers dnaG-For (5′-CATGCCATGGGGAGATTTAATTTGCG AATATGATC-3′) and dnaG-Rev (5′-GGAATTCAAATCACATGCTACATG CGTTC-3′). The primers contained NcoI and EcoRI restriction enzyme cloning sites in their 5′ and 3′ regions, respectively (underlined). The gene was cloned downstream of the *lac* promoter and glutathione *S*-transferase (GST)-tag coding sequence in vector pET41a+ (Novagen, Madison, WI) and transformed into *E. coli* BL21(DE3) (Novagen, Madison, WI). The cloned insert was sequenced in both directions by the University of Nebraska Medical Center Eppley Molecular Biology Core Facility to verify content.

Construction of plasmid for the expression of recombinant *S. aureus* DnaC. The coding sequence for *dnaC* from *S. aureus* sp. strain N315 was amplified by PCR using primers dnaC-For (5′-AAGAGGTGTAACCATCCATGGATAG-3′) and dnaC-Rev (5′-TGCAAATAAAACTCGAGCATTGATTTTC-3′). The primers contained NcoI and XhoI restriction enzyme cloning sites in their 5′ and 3′ regions, respectively (underlined). The gene was cloned downstream of the *lac* promoter in vector pET19b+ (Novagen, Madison, WI) and transformed into *E. coli* BL21(DE3) (Novagen, Madison, WI). The cloned insert was sequenced in both directions by the University of Nebraska Medical Center Eppley Molecular Biology Core Facility to verify content.

Expression and purification of *S. aureus* and *E. coli* DnaG primases. For the production of recombinant *S. aureus* DnaG, *E. coli* BL21(DE3) (pET41a+::*dnaG*) was grown in 4 liters of 2×YT medium containing 50 μg of kanamycin per ml at 30°C, with shaking at 200 rpm. When the culture reached an optical density at 600 nm of 1.0, 0.5 mM IPTG (isopropyl-β-D-thiogalactopyranoside) was added, and the induced cells were grown for 2 h. Cultures were centrifuged at 5,000 × *g* for 15 min at 4°C, and the cell pellets (15.5 g wet weight) were resuspended in 46.5 ml of lysis buffer containing 50 mM Tris, 5 mM EDTA, 0.4 mM phenylmethylsulfonyl fluoride, 0.5% Triton X (pH 8.0), and 15 mg of lysozyme. Cells were broken by four freeze-thaw cycles followed by homogenization on ice. Soluble cell extracts were obtained by centrifugation at 12,000 × *g* for 30 min at 4°C, and lysates were applied to a 5-ml bed volume of glutathione Sepharose column (Novagen, Madison, WI). The column was washed three times with 15 ml of 50 mM Tris (pH 8.0), and the enzyme was eluted from the column with 15 ml of 50 mM Tris containing 5 mM reduced glutathione (pH 8.0). The enzyme was then loaded onto a 5 ml MonoQ anion exchange column (Bio-Rad, Hercules, CA). A 0 to 1 M NaCl gradient was used to elute the enzyme, and the fractions containing primase were concentrated using a Vivaspin 15R concentrator (Vivascience, Hannover, Germany). *E. coli* DnaG was isolated as previously described (8) from a primase-overproducing strain kindly supplied by Roger McMacken (John Hopkins University). Enzyme purity and subunit molecular mass were estimated by sodium dodecyl sulfate-polyacrylamide gel electrophoresis. The concentrations of *S. aureus* and *E. coli* primase were determined using monomer extinction coefficients of 87,840 M^{-1} cm^{-1} and 47,800 M^{-1} cm^{-1}, respectively, at 280 nm.

Expression and purification of *S. aureus* and *E. coli* replicative helicases. For the production of recombinant *S. aureus* DnaC helicase, *E. coli* BL21(DE3) (pET19b+::*dnaC*) was grown at 30°C with shaking at 250 rpm in 2 liters of LB medium containing 50 μg of ampicillin, 20 μg thiamine, and 5 mg glucose per ml. When the culture reached an optical density at 600 nm of 0.8, 0.4 mM IPTG (isopropyl-β-D-thiogalactopyranoside) was added and the induced cells were grown for 2 h. Cultures were centrifuged at 5,000 × *g* for 15 min at 4°C, and the cell pellets (16.2 g wet weight) were resuspended in 48.6 ml of lysis buffer containing 50 mM Tris, 5 mM EDTA, 0.4 mM phenylmethylsulfonyl fluoride, 0.5% Triton X, 250 mM NaCl (pH 8.0), and 16 mg lysozyme. Cells were broken by three cycles of sonication, and the insoluble fraction was collected by centrifugation at 12,000 × *g* for 30 min at 4°C. The DnaC was made soluble by incubating the pellet with 5 ml of 50 mM Tris–2 mM $MgCl_2$–2 mM ATP (pH 8.0) for 20 min on ice. The suspension was cleared by centrifugation at 12,000 × *g* for 30 min at 4°C. The protein solution was then loaded onto a 5 ml MonoQ anion exchange column (Bio-Rad, Hercules, CA), and a 0 to 1 M NaCl gradient was used to elute the enzyme. Fractions containing helicase were concentrated using a Vivaspin 15R concentrator (Vivascience, Hannover, Germany). *E. coli* DnaB helicase was isolated using a procedure similar to that described for *E. coli* DnaG primase (11); pRLM1038, the *E. coli* helicase expression plasmid, was generously provided by Roger McMacken. Enzyme purity and subunit molecular mass were estimated by sodium dodecyl sulfate-polyacrylamide gel electrophoresis. The concentration of *S. aureus* helicase was determined using the method of Bradford (4), and the *E. coli* helicase concentration was determined using the hexamer extinction coefficient of 185,000 M^{-1} cm^{-1} at 280 nm.

RNA primer synthesis. Reactions were carried out using previously optimized conditions. Briefly, the reaction mixtures were incubated at 30°C in nuclease-free buffer (50 mM HEPES [pH 7.5], 5 mM potassium glutamate, 10 mM dithiothreitol) containing 10 mM magnesium acetate, a 200 or 400 μM concentration of each ribonucleotide, and the indicated amount of ssDNA template and primase either without or with helicase (800 nM). RNA primer synthesis was quenched by desalting the reaction in a Sephadex G-25 spin column.

RNA primer analysis. The primase reaction products were subjected to thermally denaturing HPLC, as previously described (12). Briefly, the reaction products were analyzed using an HPLC column that separated the nucleic acids by size and hydrophobicity. Nucleic acids were detected and quantitated spectrophotometrically at 260 nm. Control single-stranded oligoribonucleotides and deoxyribonucleotides were used to correlate retention time on the column with the sequence of the nucleic acid species. All experiments were performed in triplicate.

Bioinformatic analysis of the *S. aureus and E. coli* genomes. The full-length nucleotide sequences of *S. aureus* N315 (NC002745) and *E. coli* K-12 (NC000913) were obtained from the GenBank database. The algorithm for identification and quantitation of skewed octamers was applied as described previously (19). The output included the 10 most overrepresented and skewed

octamers along with their frequencies and percentages of skew toward the strand of DNA that serves as the lagging-strand template.

RESULTS

The first goal of this study was to determine *S. aureus* primase initiation specificity and whether it correlated with the *S. aureus* genome signature. The second goal of this study was to determine whether one bacterial replication fork helicase was capable of stimulating another bacteria's primase activity.

Expression of *S. aureus* DnaG primase and DnaC helicase. The putative *S. aureus* primase *dnaG* gene was identified within the genome of N315 (NC002745) and was cloned using standard PCR methods. All attempts to overexpress DnaG in *E. coli* using a variety of conditions resulted in an insoluble product. Therefore, since GST fusion proteins have been reported to improve recombinant protein solubility and have been used successfully in studies of other DNA-binding proteins (10), *dnaG* was cloned and expressed as a GST fusion protein. The N-terminal GST tag on *S. aureus* primase allowed for purification using affinity chromatography followed by ion-exchange chromatography. The replicative helicase *dnaC* gene from *S. aureus* sp. strain N315 was also amplified and cloned using standard procedures. Expression of *S. aureus* DnaC in *E. coli* resulted in an insoluble product that was then solubilized with magnesium ion and ATP and purified using ion-exchange chromatography. Enzyme purity and subunit molecular mass for both *S. aureus* DnaG and DnaC were estimated by sodium dodecyl sulfate-polyacrylamide gel electrophoresis. The molecular masses for the GST-tagged DnaG and untagged DnaC were 102 kDa and 53 kDa, respectively (Fig. 1). Both of these values correspond to the predicted molecular masses. After isolation, both proteins were more than 98% pure. The final yield was 2 mg of *S. aureus* primase and 10 mg of *S. aureus* helicase per liter of culture.

Proteolytic cleavage of the GST tag from primase, as well as expression of an untagged protein, resulted in an insoluble protein under a wide variety of conditions. Therefore, the primase fusion protein was tested for in vitro activity using a previously developed RNA primer synthesis assay in conjunction with an HPLC detection method (12). The assay was developed to determine the quantity and length of all RNA primers. The ability of the purified enzyme to generate primers de novo was determined using a 23-mer synthetic ssDNA template in a reaction mixture containing ribonucleoside triphosphates (rNTPs) and magnesium ion. For uniformity of analysis, the ssDNA template backbone used in previous studies with *E. coli* primase was utilized.

Bioinformatic analysis of overrepresented octamers in *S. aureus*. Computational analysis of the complete DNA sequences of *S. aureus* N315 and *E. coli* K12 was performed using a previously defined algorithm that tabulated the nonrandom overrepresentation of sequences eight nucleotides in length (octamers) (19). The most abundant octamers and their skew toward the lagging-strand DNA template were calculated. The nine most frequently occurring octamers in *S. aureus* contained the trinucleotide TTA (Table 1A), whereas in *E. coli* eight of the skewed octamers contained the trinucleotide CTG (Table 1B). None of the overrepresented *S. aureus* octamers contained any known chi sequences. In contrast, the *E. coli*

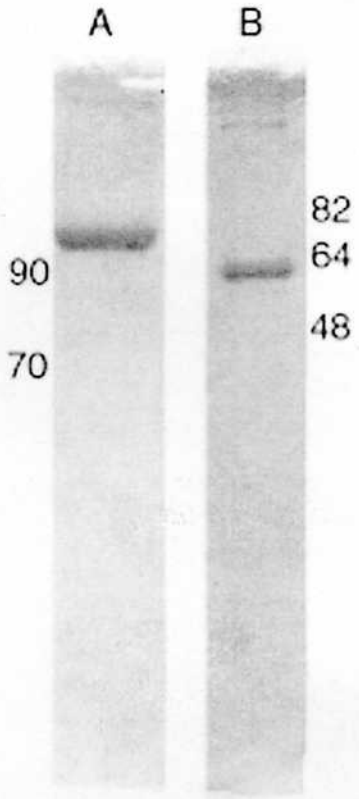

FIG. 1. Purity analysis of recombinant *S. aureus* DnaG primase and DnaC helicase. Sodium dodecyl sulfate–10% polyacrylamide gel electrophoresis analysis of 5 μg of purified primase (A) or helicase (B). The locations of the molecular mass markers (in kilodaltons) are indicated next to the respective gel photograph.

octamers were found to be permutations of the chi octamer (GCTGGTGG), as previously described (3).

Trinucleotide initiation specificity of *S. aureus* primase. To investigate a possible relationship between genome content and the preferred primase recognition sequence, the ssDNA templates listed in Table 2 were synthesized. These templates contained the previously defined minimal structural elements necessary to support primer synthesis by *E. coli* primase and provided for testing of all the possible trinucleotide motifs contained within the overrepresented octamers listed in Table 1 (22). In addition, since leucine is the most abundant amino acid found in proteins expressed by both *E. coli* and *S. aureus*, all trinucleotides that encode for leucine were assessed. Several trinucleotides present in the proposed *OriC* of *S. aureus* (13) as well as remaining trinucleotides that complete the NTA series were also examined in the *S. aureus* primase activity assays.

Primase, magnesium ion, and rNTPs were incubated with the various templates, and the reactions were analyzed by HPLC to determine whether any of the ssDNA templates shown in Table 2 supported RNA primer synthesis. *E. coli* primase was used in control reactions with an oligonucleotide template containing the initiation trinucleotide CTG (2). Unlike the findings for *E. coli*, *S. aureus* primase was capable of producing specific and appropriately sized RNA primers from

TABLE 1. Computational analysis of overrepresented and skewed octamers found in the genomes of *S. aureus* strain N315 and *E. coli* strain K-12[a]

Rank	*S. aureus* strain N315 result			*E. coli* strain K-12 result		
	Octamer	No. of occurrences	% Skew	Octamer	No. of occurrences	% Skew
1	tTTAaaat	1,494	59.2	tgCTGgcg	1,511	58.4
2	tTTAtttt	1,486	59.8	ggcgCTGg	1,388	60.3
3	tTTAattt	1,319	61.8	tgCTGgcg	1,317	56.5
4	TTAatttt	1,315	57.7	gCTGgcgg	1,275	57.7
5	tttTTAtt	1,283	57.2	gCTGgcgc	1,180	56.5
6	ttTTAttt	1,268	58.3	gcgCTGgc	1,179	58.9
7	tttTTAat	1,233	57.9	tggcgCTG	1,176	58.6
8	ttTTAatt	1,225	58.9	TGcgccag	1,020	56.8
9	TTAatttt	1,223	56.6	Gccgccag	1,019	58.3
10	atatttTT	1,221	60.2	gCTGgtgg	1,008	75.7

[a] The 10 most frequently occurring skewed octamers are listed in the order of frequency of occurrence as calculated using a previously described algorithm. The total count for each octamer and the skew percentage for each octamer are listed. The octamers are aligned according to the TTA motif in *S. aureus* and the CTG motif in *E. coli*.

templates containing either the trinucleotide CTA or TTA (Table 2 and Fig. 2). Templates containing the trinucleotide GTA produced only a small amount of RNA primer product (Table 2 and Fig. 2). The area of the RNA polymer peaks was calculated to determine the relative amounts of primers synthesized. The template containing CTA resulted in the largest amount of primer product (131.1 mV·min), with the template containing TTA being the next best trinucleotide sequence to result in a high quantity of RNA polymers (57.3 mV·min). The GTA-containing template resulted in the least amount of primer production by *S aureus* DnaG (16.3 mV·min). None of the other templates tested produced a detectable amount of primer product (Table 2).

The major RNA polymers synthesized by *S. aureus* primase eluted at 8.05 min and 8.48 min with ssDNA templates containing CTA and TTA, respectively (Fig. 2). The elution time for these two RNA primers, both 16 nucleotides in length but differing in composition by a single nucleotide, corresponded to the expected elution time based on our previous studies, which were determined using control oligomers with various hydrophobicity (12). Less-abundant and shorter RNA primers were also generated that eluted at 7.72, 7.44, 7.27, 6.89, 6.05, and 5.90 min with the CTA template and 8.17, 7.90, 7.75, and 7.43 min with the TTA template, corresponding to a series of smaller products that progressively differed by one fewer nucleotide.

Additional templates containing mutations of the second or third base within the CTA or TTA trinucleotide were generated and tested in the primase activity assay. Use of these templates resulted in undetectable levels of primer products (Table 2). These data showed that both the second and third nucleotides in the recognition sequence were essential for *S. aureus* primer initiation. As an important control for these studies, *S. aureus* primase activity exhibited no activity in a

TABLE 2. ssDNA oligonucleotides (templates) showing their ability to support DNA-dependent RNA synthesis activity by recombinant *S. aureus* primase[a]

Template	Primer synthesis	Template	Primer synthesis
AAA	−	CTG	−
AAG	−	CTT	−
AAT	−	GAA	−
ATA	−	GTA	+
ATC	−	TAA	−
ATT	−	TAG	−
CAG	−	TAT	−
CAT	−	TTA	++
CGA	−	TTC	−
CTA	+++	TTG	−
CTC	−	TTT	−

[a] Templates of the format 5′-CAGA$(CA)_5$ XYZ $(CA)_3$-3′, where XYZ is the trinucleotide listed in the table were tested for their ability (+++, ++, or +) or inability (−) to support RNA primer synthesis. The reactions were performed using 200 nM template, 2 μM primase, and 200 μM rNTPs during a 1 h incubation at 30°C.

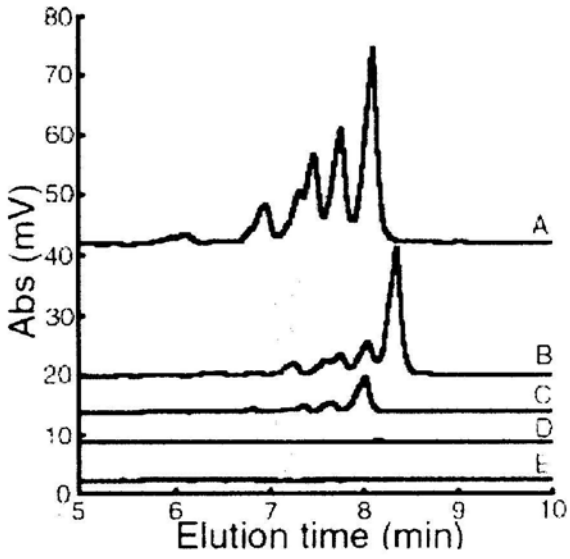

FIG. 2. Representative chromatograms of primase activity on ssDNA templates. Denaturing HPLC analysis was performed on the RNA products derived from *S. aureus* primase activity on templates containing the trinucleotide CTA (A), TTA (B), GTA (C), ATA (D), or CTG (E). The reactions were performed using 2 μM template, 2 μM primase, and 400 μM rNTPs during a 1-h incubation at 30°C. Abs, absorbance at 260 nm.

reaction using the template containing CTG, the trinucleotide initiation sequence for *E. coli* primase (Fig. 2). Overall, these experiments demonstrated that the observed activity of *S. aureus* primase was specific and not due to a contaminant derived from the *E. coli* strain used for recombinant protein expression.

Identification of the initial ribonucleotide in the primers synthesized by *S. aureus DnaG*. Previous studies showed that RNA primers generated by *E. coli* primase are initiated complementarily to the middle T in the CTG template (11). To identify whether the RNA primer synthesized by the *S. aureus* DnaG initiated complementarily to the middle T in the TTA embedded within the ssDNA template, a series of reactions were performed using progressively lower amounts of rCTP. Since the template contained only one guanosine located in the antepenultimate position, primer synthesis initiating complementarily to the middle T of the trinucleotide TTA should generate a 16-mer RNA primer eluting at 8.48 min, as illustrated in Fig. 3A. However, in the absence of rCTP, primer synthesis would stall before the antepenultimate position and result in a 13-mer RNA primer (Fig. 3A).

In the absence of rCTP, *S. aureus* primase created one major primer species that eluted at 7.75 min., corresponding with a 13-mer RNA species (Fig. 3B) (12). As rCTP was titrated into the reaction, the 13-mer peak disappeared and a new 8.48 min peak consistent with a 16-mer became the dominant primer species. A similar experiment was performed using *S. aureus* primase and the template containing the trinucleotide CTA. These results also demonstrated that the full-length primer was a 16-mer in the presence of rCTP and that, in the absence of rCTP, a 13-mer primer product was the major RNA polymer synthesized (data not shown). In the absence of rATP, no RNA product was observed for either the CTA- or TTA-containing templates. These results confirmed that the RNA primer initiates complementarily to the middle T in both of these trinucleotide templates and that the third nucleotide in the initiation sequence serves an essential but cryptic function.

Helicase stimulation of primase. The replicative *E. coli* helicase (DnaB) has been shown to stimulate the synthesis of RNA primers by *E. coli* primase and to release *E. coli* primase specificity for the trinucleotide CTG (11). Thus, in the presence of helicase, *E. coli* primase is capable of generating primers from a variety of templates. To determine whether DnaC (an *E. coli* DnaB ortholog), the *S. aureus* replicative helicase, would also stimulate *S. aureus* primase DnaG activity, *S. aureus* primase activity assays in the presence or absence of *S. aureus* DnaC were performed using a low concentration of primase (400 nM) and either the CTA or TTA templates. Note that this primase concentration was much less than the 2.0 μM used as described above for *S. aureus* primase (Fig. 2). The concentration was intentionally reduced to a level that would generate a visible product when helicase was added at 800 nM for helicase monomer (see Fig S1 in the supplemental material). The addition of *S. aureus* helicase DnaC stimulated *S. aureus* primase DnaG activity by 2.7-fold with the CTA template and by 1.6-fold with the TTA template (Fig. 4). The predominant RNA polymer for both templates was the full-length 16-mer. Moreover, the stimulatory effect of the helicase on *S. aureus* primase activity did not release primase initiation specificity, since templates other than those containing CTA or TTA did not result in a detectable primer product (data not shown). These results demonstrated that the interaction of *S. aureus* helicase with the *S. aureus* primase resulted in stimulation of predominately full-length primer synthesis in the presence of the appropriate initiation template.

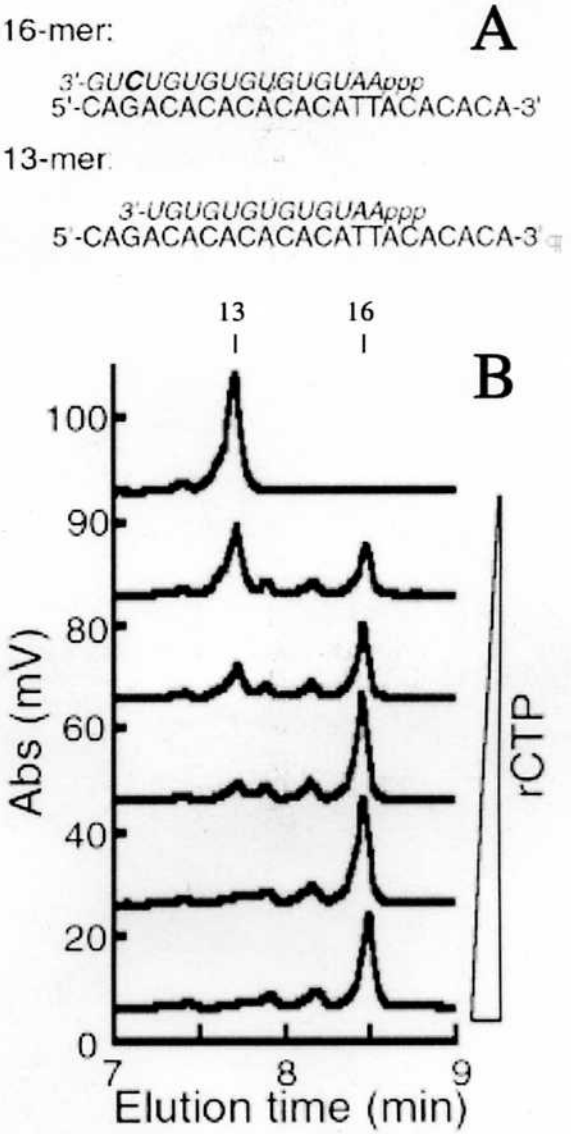

FIG. 3. Determination of the RNA primer initiation site on the TTA template for *S. aureus* primase. (A) Schematics of the predicted RNA primer product (italics) in either the presence or absence of rCTP (bold) on the ssDNA template. (B) Denaturing HPLC analysis of RNA primer synthesis in the presence of 0, 25, 50, 100, 200, and 400 μM rCTP. The reactions were performed using 2 μM ssDNA template, 2 μM primase, and 400 μM rNTPs during a 1-h incubation at 30°C. Abs, absorbance at 260 nm.

Restricted helicase stimulation of primase. To determine whether helicase stimulation of primase was restricted at the genus level, the ability of *E. coli* DnaB helicase to stimulate *S. aureus* primase, as well as the ability of *S. aureus* DnaC helicase to stimulate *E. coli* primase, was tested. In reactions using a low concentration of primase (400 nM), *S. aureus* primase

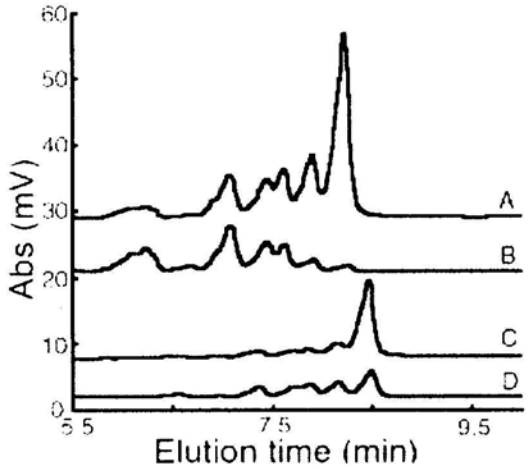

FIG. 4. Stimulatory effect of *S. aureus* replicative helicase on *S. aureus* primase activity. Denaturing HPLC analysis was performed on the RNA products derived from *S. aureus* primase activity on templates containing the trinucleotide CTA with helicase (A) and without helicase (B) or the trinucleotide TTA with helicase (C) and without helicase (D). *S. aureus* DnaG primase (400 nM) was incubated for 1 h with 400 μM rNTPs and 2 μM ssDNA without or with *S. aureus* DnaC helicase (800 nM). Abs, absorbance at 260 nm.

produced a detectable amount of RNA primers whereas *E. coli* primase did not (Fig. 5). The amount of *E. coli* primase used in this assay was much lower than in an earlier study (12). It was reduced to a level that would generate a visible product when helicase was added. The addition of *E. coli* DnaB helicase stimulated *E. coli* DnaG activity that resulted in primers shorter than the expected 16-mer that averaged 12 bases in length (Fig. 5), similar to the findings in previous studies (11). *S. aureus* DnaC helicase stimulated the production by *S. aureus* DnaG of full-length RNA polymers 16 bases in length but did not produce an observable change in *E. coli* primase activity. Similarly, *E. coli* DnaB helicase stimulated only *E. coli* primase activity and not *S. aureus* primase activity. Notably, the addition of *E. coli* DnaB helicase inhibited the basal level of *S. aureus* DnaG activity. Collectively, these results showed that *S. aureus* DnaC substantially stimulated *S. aureus* primase activity and that this stimulatory effect differed from that observed for *E. coli* primase and helicase interactions. More specifically and in contrast to the findings for *E. coli*, *S. aureus* helicase stimulation of *S. aureus* DnaG did not shorten the length of the RNA primers synthesized and primase initiation specificity was not released. In addition, these data demonstrated that for both *E. coli* and *S. aureus*, the helicase interaction with primase was not cross-reactive.

DISCUSSION

***S. aureus* DnaG primase recognition sequence and stimulation by helicase.** Bacterial genomes are constantly being exposed to a variety of plasmids and other foreign DNA. A mechanism to protect the genome from replicating nonnative DNA may convey a selective advantage to the species. The studies described here identified a number of important distinctions between *E. coli* and *S. aureus* related to DNA replication, including different initiation sequences and primase-helicase interactions restricted to each bacterial species. Unlike *E. coli* primase, which initiates de novo primer synthesis on templates containing the trinucleotide CTG, *S. aureus* primase synthesized an RNA primer predominately on templates containing CTA or TTA and to a much lesser degree on GTA-containing templates. The results of the cytosine titration studies in *S. aureus* were consistent with previous findings for *E. coli* with the RNA primer initiating complementarily to the middle T in the trinucleotide-containing template and the third nucleotide in the recognition trinucleotide serving as a cryptic nucleotide that is essential for efficient primer formation (6).

A second level of restriction at the genus level was found in

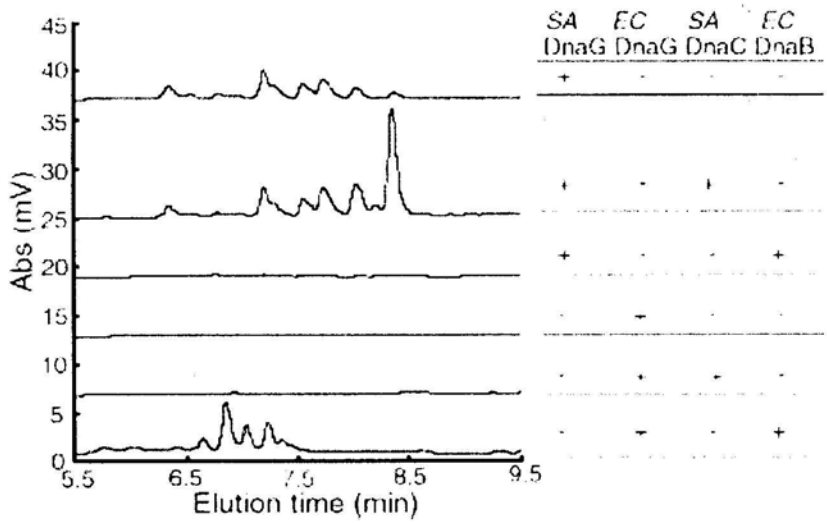

FIG. 5. Cross-species effect of replicative helicase stimulation on primase activity. *S. aureus* or *E. coli* primase (400 nM) was incubated for 30 min with 400 μM rNTPs, 2 μM ssDNA, and *S. aureus* or *E. coli* helicase (800 nM). The reaction products were analyzed by denaturing HPLC. The ssDNA template contained the TTA trinucleotide in *S. aureus* primase reactions and the CTG trinucleotide in the *E. coli* primase reactions. Abs, absorbance at 260 nm.

the interaction between primase and helicase. More specifically, helicase from *E. coli* was unable to stimulate *S. aureus* primase activity and *S. aureus* helicase was incapable of stimulating *E. coli* primase in our system. These findings contrast with findings obtained with the subunits of the *S. aureus* PolC and *E. coli* polymerase III holoenzymes, which have been demonstrated to be generally interchangeable (5).

Interestingly, most bacteriophages encode their own primase and helicase, indicating that the host primase and helicase are unable to support replication of the phage genome. Despite the likelihood that eubacterial primases and helicases from different species have the same overall structure, differences in key residues may have evolved to prevent the primase and/or helicase from functioning on nonnative replication forks, such as those found with invading bacteriophages. For example, several residues in *G. stearothermophilus* DnaB helicase that are not conserved in *E. coli* DnaB have been recently identified to have an important role in mediating protein-protein interactions required for helicase modulation of primase activity (23).

Correlation of genome content and primase initiation specificity. For over 10 years bacterial genomes have been known to contain certain oligonucleotides that are overrepresented or skewed (18). The biologic significance of this phenomenon, however, remains a matter of significant debate. A variety of asymmetrical pressures could contribute to overrepresentation of a particular sequence on either DNA strand, including recombination and repair, composition strand bias, DNA replication, and codon bias. In agreement with other studies (1, 24), our data do not support the recombination-repair hypothesis as a basis for generation of overrepresented oligonucleotides. Our studies demonstrated that the preferred recognition sequence for *S. aureus* primase was different from the recognition sequence for *E. coli*. However, in both genomes a functional primase recognition sequence was present within the most frequently occurring octamers.

Codon bias may partially explain overrepresentation of the TTA-containing octamers in *S. aureus* and the CTG-containing octamers in *E. coli*. In both organisms, leucine is the most abundant amino acid within synthesized proteins and the most biased codons for leucine are TTA in *S. aureus* and CTG in *E. coli* (see the codon usage table for *Staphylococcus aureus* N315 and *Escherichia coli* K-12 at the website for The Institute for Genomic Research [http://www.tigr.org]). However, the skewed octamers are not preferentially located in coding versus noncoding regions of the genome (19, 20). Therefore, codon bias and amino acid usage cannot fully explain the basis for the genomic signatures observed.

While TTA was overrepresented on the lagging-strand template, the other significant *S. aureus* primase initiation trinucleotide, CTA, was not. One possible explanation is that the evolution of an AT-rich genome in *S. aureus* required DnaG primase to adapt accordingly, with TTA representing a more biologically appropriate initiation sequence given the abundance of this trinucleotide in the genome. Another possibility is that TTA is the most-utilized primase initiation sequence during routine DNA synthesis and that CTA serves as the primase template during specialized conditions such as during the initiation of the replication fork or during DNA repair. Alternatively, the initial two ribonucleotides in the primer product, specifically 5′-pppApG-3′, and/or the pyrimidine-pyrimidine-purine recognition sequence on the template has been conserved due to common structural or conformational constraints within the recognition-active site of bacterial primase. Ongoing structural studies should facilitate determination of the precise mechanism for *S. aureus* primase recognition of specific initiation trinucleotides and subsequent de novo synthesis of short RNA polymers.

Bidirectional replication from a single origin produces a finite limit on prokaryotic DNA replication time (17). When all other features are constant, long genomes take longer to replicate. If cell duplication rates are an important component of fitness, then single origins favor small genomes and the elimination of nonuseful DNA. We propose here that single origins of bidirectional replication also favor a uniform overabundance of primase initiation sequences on the lagging-strand template. When the primase initiation sequences are sufficiently abundant, the DNA replication rate is limited by other factors, such as deoxynucleoside triphosphate pools, DNA polymerase subunit concentrations, fork helicase concentration, SSB, rNTP pools, and primase concentration (25, 26). However, in an exponentially growing cell none of these factors varies. So, for those portions of the genome in which the primase initiation sequence is rare, the replication rate will slow down and will be limited by the rate of primase initiation, the rate-limiting step for primer synthesis. In this way, primase specificity exerts selective pressure on the genome sequence to maintain an abundance of initiation sequences on the lagging-strand template.

In a search for new sequence elements within a single strand of the *E. coli* genome, the Blattner laboratory counted the abundance of every octanucleotide sequence (3). They found that the overabundant sequences were GC rich, crossed from one strand to the other at the replication origin and terminus, and occurred with higher frequency than the average Okazaki fragment length. Most of these sequences contained the CTG trinucleotide and were preferentially found on the strand that is the lagging-strand template. Since the overrepresented sequences cross over at the origin and terminus, these sequences are related to the replication process. Since *E. coli* primase preferentially initiates from CTG, they suggested that the function of these sequences was to promote primer initiation. This correlation provides a mechanism for primase to select for the maintenance of these overrepresented sequences and further suggests another mechanism to constrain lateral gene transfer between distantly related species.

Primase and helicase interactions in other bacteria and genomic signatures. Our study of *S. aureus* primase initiation specificity and modulation by helicase has identified at least two issues that will require further investigation. Since *E. coli* and *S. aureus* are representatives of the distantly related families of gram-negative and gram-positive bacteria, further studies with other bacterial enzymes will establish whether the relationship between genome content and primase recognition sequence is universal. Although the majority of bacterial genomes are expected to have overrepresented and strand-skewed oligonucleotides, the primase recognition sequence has only been determined for a few bacteria (18, 19). The recognition sequences for *G. stearothermophilus* primase have been recently reported to be CTA and TTA, as with our findings for *S. aureus*, but the initiating nucleotide appears to be different

(23). Since the genomic sequence of *G. stearothermophilus* has not been determined, a correlation between the *G. stearothermophilus* DnaG initiation sequences and genome content cannot currently be evaluated. The second question requiring further study is whether the specific stimulatory effect of helicase on primase will be restricted at the species level or will have a general effect among all gram-positive organisms. These issues are important because it may be possible to exploit the close relationship between primase and helicase and the potential differences in activity at the species or group level for new therapeutic drug discovery.

Specific strategies for antibiotic development have been proposed based on the essentiality and divergence of the eubacterial primases from their eukaryotic counterparts and the key interactions between primase and replicative helicases (21). X-ray crystallography of portions of the enzymes believed to be involved in the stimulation of primase by helicase has identified a variety of sites for targeting inhibitory chemicals. Our findings suggest that inhibitors of primase-helicase interactions will probably have narrower activity than inhibitors of DNA binding by primase.

ACKNOWLEDGMENTS

This work was supported in part by a grant from the Department of Defense, Defense Advanced Research Program Agency (award W911NF0510275).

We thank Dhundy Bastola and Khalid Sayood for assistance with genome sequence analysis.

REFERENCES

1. **Bell, S. J., Y. C. Chow, J. Y. Ho, and D. R. Forsdyke.** 1998. Correlation of chi orientation with transcription indicates a fundamental relationship between recombination and transcription. Gene **216:**285–292.
2. **Bhattacharyya, S., and M. A. Griep.** 2000. DnaB helicase affects the initiation specificity of *Escherichia coli* primase on single-stranded DNA templates. Biochemistry **39:**745–752.
3. **Blattner, F. R., G. Plunkett III, C. A. Bloch, N. T. Perna, V. Burland, M. Riley, J. Collado-Vides, J. D. Glasner, C. K. Rode, G. F. Mayhew, J. Gregor, N. W. Davis, H. A. Kirkpatrick, M. A. Goeden, D. J. Rose, B. Mau, and Y. Shao.** 1997. The complete genome sequence of *Escherichia coli* K-12. Science **277:**1453–1474.
4. **Bradford, M. M.** 1976. A rapid and sensitive method for the quantitation of microgram quantities of protein utilizing the principle of protein-dye binding. Anal. Biochem. **72:**248–254.
5. **Bruck, I., R. E. Georgescu, and M. O'Donnell.** 2005. Conserved interactions in the *Staphylococcus aureus* DNA PolC chromosome replication machine. J. Biol. Chem. **280:**18152–18162.
6. **Frick, D. N., and C. C. Richardson.** 2001. DNA primases. Annu. Rev. Biochem. **70:**39–80.
7. **Griep, M. A.** 1995. Primase structure and function. Indian J. Biochem. Biophys. **32:**171–178.
8. **Griep, M. A., and E. R. Lokey.** 1996. The role of zinc and the reactivity of cysteines in *Escherichia coli* primase. Biochemistry **35:**8260–8267.
9. **Grompe, M., J. Versalovic, T. Koeuth, and J. R. Lupski.** 1991. Mutations in the *Escherichia coli dnaG* gene suggest coupling between DNA replication and chromosome partitioning. J. Bacteriol. **173:**1268–1278.
10. **Howell, L. D., R. Borchardt, J. Kole, A. M. Kaz, C. Randak, and J. A. Cohn.** 2004. Protein kinase A regulates ATP hydrolysis and dimerization by a CFTR (cystic fibrosis transmembrane conductance regulator) domain. Biochem. J. **378:**151–159.
11. **Johnson, S. K., S. Bhattacharyya, and M. A. Griep.** 2000. DnaB helicase stimulates primer synthesis activity on short oligonucleotide templates. Biochemistry **39:**736–744.
12. **Koepsell, S., D. Bastola, S. H. Hinrichs, and M. A. Griep.** 2004. Thermally denaturing high-performance liquid chromatography analysis of primase activity. Anal. Biochem. **332:**330–336.
13. **Kuroda, M., T. Ohta, I. Uchiyama, T. Baba, H. Yuzawa, I. Kobayashi, L. Cui, A. Oguchi, K. Aoki, Y. Nagai, J. Lian, T. Ito, M. Kanamori, H. Matsumaru, A. Maruyama, H. Murakami, A. Hosoyama, Y. Mizutani-Ui, N. K. Takahashi, T. Sawano, R. Inoue, C. Kaito, K. Sekimizu, H. Hirakawa, S. Kuhara, S. Goto, J. Yabuzaki, M. Kanehisa, A. Yamashita, K. Oshima, K. Furuya, C. Yoshino, T. Shiba, M. Hattori, N. Ogasawara, H. Hayashi, and K. Hiramatsu.** 2001. Whole genome sequencing of methicillin-resistant *Staphylococcus aureus*. Lancet **357:**1225–1240.
14. **Liu, J., M. Dehbi, G. Moeck, F. Arhin, P. Bauda, D. Bergeron, M. Callejo, V. Ferretti, N. Ha, T. Kwan, J. McCarty, R. Srikumar, D. Williams, J. J. Wu, P. Gros, J. Pelletier, and M. DuBow.** 2004. Antimicrobial drug discovery through bacteriophage genomics. Nat. Biotechnol. **22:**185–191.
15. **Oakley, A. J., K. V. Loscha, P. M. Schaeffer, E. Liepinsh, G. Pintacuda, M. C. Wilce, G. Otting, and N. E. Dixon.** 2005. Crystal and solution structures of the helicase-binding domain of *Escherichia coli* primase. J. Biol. Chem. **280:**11495–11504.
16. **Pan, H., and D. B. Wigley.** 2000. Structure of the zinc-binding domain of *Bacillus stearothermophilus* DNA primase. Structure Fold. Des. **8:**231–239.
17. **Poole, A. M., M. J. Phillips, and D. Penny.** 2003. Prokaryote and eukaryote evolvability. Biosystems **69:**163–185.
18. **Rocha, E. P.** 2004. The replication-related organization of bacterial genomes. Microbiology **150:**1609–1627.
19. **Salzberg, S. L., A. J. Salzberg, A. R. Kerlavage, and J. F. Tomb.** 1998. Skewed oligomers and origins of replication. Gene **217:**57–67.
20. **Sandberg, R., C. I. Branden, I. Ernberg, and J. Coster.** 2003. Quantifying the species-specificity in genomic signatures, synonymous codon choice, amino acid usage and G+C content. Gene **311:**35–42.
21. **Soultanas, P.** 2005. The bacterial helicase-primase interaction: a common structural/functional module. Structure (Cambridge) **13:**839–844.
22. **Swart, J. R., and M. A. Griep.** 1993. Primase from *Escherichia coli* primes single-stranded templates in the absence of single-stranded DNA-binding protein or other auxiliary proteins. Template sequence requirements based on the bacteriophage G4 complementary strand origin and Okazaki fragment initiation sites. J. Biol. Chem. **268:**12970–12976.
23. **Thirlway, J., and P. Soultanas.** 2006. In the *Bacillus stearothermophilus* DnaB-DnaG complex, the activities of the two proteins are modulated by distinct but overlapping networks of residues. J. Bacteriol. **188:**1534–1539.
24. **Uno, R., Y. Nakayama, K. Arakawa, and M. Tomita.** 2000. The orientation bias of Chi sequences is a general tendency of G-rich oligomers. Gene **259:**207–215.
25. **Zechner, E. L., C. A. Wu, and K. J. Marians.** 1992. Coordinated leading- and lagging-strand synthesis at the *Escherichia coli* DNA replication fork. II. Frequency of primer synthesis and efficiency of primer utilization control Okazaki fragment size. J. Biol. Chem. **267:**4045–4053.
26. **Zechner, E. L., C. A. Wu, and K. J. Marians.** 1992. Coordinated leading- and lagging-strand synthesis at the *Escherichia coli* DNA replication fork. III. A polymerase-primase interaction governs primer size. J. Biol. Chem. **267:**4054–4063.

Staphylococcus aureus Primase Is Less Stimulated by Its Helicase than *Escherichia coli* Primase

Scott A. Koepsell,[1,2] Marilynn A. Larson,[1,2] Christopher A. Frey,[2,3] Steven H. Hinrichs,[1,2] and Mark A. Griep[2,3]*

Department of Microbiology and Pathology, University of Nebraska Medical Center, Omaha, Nebraska 68198-6495[1]*; University of Nebraska Center for Biosecurity, Omaha, Nebraska 68198-6495*[2]*; and Department of Chemistry, University of Nebraska-Lincoln, Lincoln, Nebraska 68588-0304*[3]

RUNNING TITLE: *S. aureus* Primase

*Corresponding author. Mailing address: Department of Chemistry, University of Nebraska-Lincoln, Hamilton Hall 614, Lincoln, NE 68588-0304. Phone: (402) 472-3429; Fax: (402) 472-9402. E-mail: mgriep1@unl.edu.

Abbreviations: DSS, disuccinimidyl suberate; DTT, dithiothreitol; GST, glutathione S-transferase from *Schistosoma japonicum*; PEG, polyethylene glycol; ssDNA, single-stranded DNA

Abstract

The study of primases from model organisms such as *Escherichia coli*, phage T7, and phage T4 has demonstrated the essential nature of primase function, which is to generate *de novo* RNA polymers to prime DNA polymerase. However, little is known about the function of primases from other eubacteria. Their low primary sequence homology may result in functional differences. To help understand which primase functions were conserved, primase and its replication partner helicase from the pathogenic Gram-positive bacteria *Staphylococcus aureus* were cloned, expressed, and purified. Its conserved properties were slow kinetics, low fidelity, poor sugar specificity, and stimulation of activity by helicase. When compared to the activity of Escherichia coli primase, however, the *S. aureus* primase had higher activity and was less stimulated by its helicase. An even more significan difference between these two primases was that the initiation specificity of *S. aureus* primase was not broadened by its interaction with its fork helicase.

Introduction

Primase is the specialized DNA-dependent RNA polymerase that generates short oligoribonucleotide polymers *de novo* elongated by DNA polymerase to initiate DNA synthesis (*1, 2*). During bacterial DNA replication on a circular chromosome, primase initiates leading strand synthesis at least once and lagging strand synthesis many times. In *Escherichia coli* and *Staphylococcus aureus*, conditionally lethal mutations in the primase genes yielded a lethal phenotype under the non-permissive conditions, demonstrating the essentiality of the enzyme (*3, 4*). The indispensable function of primase and the structural divergence of the eukaryotic and prokaryotic primases (*5, 6*) have lead to the identification of the enzyme as a target for novel antibiotic development (*7, 8*).

An important consideration for using primase as an antibiotic target is whether or not the low primary sequence homology among the eubacterial primases has any functional relevance. The *E. coli* DnaG gene product is the model eubacterial primase because its structure and function have been extensively characterized. It has been demonstrated that the *E. coli* primase is slow (*9*), has low-fidelity (*9*), binds G4-ori ssDNA as a dimer (*10, 11*), and that DnaB helicase stimulates its catalytic activity over 15-fold (*12*). *E. coli* primase specifically initiates RNA primer synthesis complementary to the trinucleotide 5'-d(CTG)-3' *in vitro* (*13*). In addition to stimulating primase activity, *E. coli* DnaB helicase has been shown to release primase initiation specificity such that most templates, even those lacking the trinucleotide d(CTG), support some measurable RNA primer synthesis *in vitro* (*13*).

The two bacterial-like primases that have been studied in the greatest biochemical detail are T7 gene 4 protein and T4 gene 61 protein (*2*). They share many similarities with *E. coli* primase including trinucleotide initiation specificity, although T7 primase recognizes d(GTC) and T4 primase recognizes d(GTT). T7 gene 4 differs significantly from the primases of T4, *E. coli* and other bacterial primases in that its N-terminus is a homologous primase but its C-terminus is a helicase that homohexamerizes. The gene 4 helicase is a homolog of bacterial DnaB helicases and the T4 gene 41 helicase. Both *E. coli* DnaB and T4 gene 41 helicase are functional homohexamers that bind and stimulate the activity of their respective primases.

Recently, it was demonstrated that the primases and replication fork helicases from mesophilic *S. aureus* and thermophilic *Geobacillus stearothermophilus* have properties that diverge from their *E. coli* homologs (*14, 15*). Both primases initiated from 5'-TTA-3' and 5'-CTA-3'. The two enzymes differed in that the fork helicase endows very little stimulation on primer synthesis activity in the *G. stearothermophilus* system but a great deal in the *S. aureus* system. In light of these findings, we investigated whether other biochemical differences might exist. The results demonstrated that *S. aureus* primase elongates with high fidelity in contrast to the low fidelity of *E. coli* primase. There was also no change in *S. aureus* primase initiation specificity was observed when stimulated by its helicase. Therefore, there are three major differences between the *S. aureus* and *E. coli* systems.

MATERIALS AND METHODS

Chemicals. HPLC-purified synthetic oligonucleotides (Table 1) were obtained from Integrated DNA Technologies (Coralville, IA). Magnesium acetate, potassium glutamate, HEPES, Brilliant Blue Colloidal stain, and DTT were obtained from Sigma (St. Louis, MO). Ribonucleoside triphosphates (NTPs) were purchased from Promega (Madison, WI). Deoxyribonucleoside (dNTPs) and dideoxynucleoside triphosphates (ddNTPs) were obtained from Roche Molecular Biosystems (Mannheim, Germany). Primer lengths and quantities were measured on a WAVE HPLC Nucleic Acid Fragment Analysis System with a DNASep HPLC column from Transgenomic (Omaha, NE).

Expression and purification of *S. aureus* primase and *S. aureus* DnaC helicase. The primase and DnaC helicase from *Staphylococcus aureus* sp. strain N315 were cloned, expressed, and purified as described (*14*). The wildtype *S. aureus* primase was prepared as the *N*-terminal GST-fusion to overcome solubility problems that were encountered in its absence. Note that *S. aureus* DnaC helicase is the ortholog of *E. coli* DnaB helicase.

Primer synthesis assay. RNA primer synthesis reactions were performed in 100 μl nuclease-free water reactions containing 50 mM HEPES, 100 mM potassium glutamate, pH 7.5, 10 mM DTT, 400 μM NTPs and 10 mM magnesium acetate. DnaC helicase (typically 133 nM hexamer) and ssDNA template (typically 2 μM) were present before the reactions were initiated with primase (typically 2 μM). The samples were incubated at 30 °C for the indicated amount of time (typically 30 to 90 min) and then quenched by heat inactivation at 65 °C for 10 min. The samples were desalted in a Sephadex G-25 spin column (Amersham, Piscataway, NJ), speed vacuumed to dryness, the pellet re-

suspended in 1/10th the original volume of water, and then 8.0 μL of the sample was analyzed by HPLC under thermally-denaturing conditions at 80 °C as previously described (*16*). The flow rate and acetonitrile gradient allowed detection of both the RNA and ssDNA template peaks, which were detected by absorbance at 260 nm. Retention time fluctuations for the RNA peaks were minimized by adjustment relative to the ssDNA template retention time.

Primer synthesis quantification. The moles of primers were quantified by using the template as an internal standard. First, the area under each RNA peak and the template peak were background-corrected and its area summed such that it had units of mV•min. Next, all areas were then divided by their relative extinction coefficients (Table 1 & 2). Finally, each reaction's template concentration was used in conjunction with its mole-adjusted area to determine the molarity (or moles) of each primer length. Total primer synthesis is reported as the sum of moles of all primer lengths. This approach also had the advantage that it eliminated the variability introduced to the system when the samples were spun, dried, resuspended, and injected.

Mathematical models. During primer synthesis, one primase binds to one template, synthesizes a short RNA polymer complementary to it, and may or may not dissociate. Therefore, the kinetic model in a pool of nucleotides is:

$$P + D \underset{k_{-1}}{\overset{k_1}{\rightleftarrows}} PD \xrightarrow{k_{cat}} PDR,$$

where P is primase, D is the ssDNA template, and R is the short RNA polymer called a primer. Since primer synthesis is the rate-limiting step, then $k_{-1} > k_{cat}$ and the K_M is essentially equal to the K_D. Therefore, as shown previously (*9*), primer synthesis is a first-order process controlled by the concentration of primase-template as $R = R_{app\ max}$ (1 -

exp($-k_{cat}$*t)), where $R_{app\ max}$ is the apparent maximum number of primers synthesized, and k_{cat} is the first-order catalytic rate (shown to be 2.4 x 10^{-4} s^{-1} below). $R_{app\ max}$ should be proportional to the PD concentration capable of priming and when the time is held constant at say 90 min, the fraction of primed templates should reach 0.726 (= 1 - *exp*(-0.00024 s^{-1} x 5400 s)). The reaction kinetics were fit to the indicated equations using Prism 4 for Macintosh (GraphPad Software, San Diego, CA).

Chemical crosslinking. The oligomeric state of the GST-primase was determined by chemical crosslinking with disuccinimidyl suberate (DSS) followed by denaturing gel electrophoresis (*17*). Each 20-μL reaction contained 4 μM GST-primase, with or without 300 μM DSS, and with or without 5 mM DTT in a buffer of 50 mM HEPES, pH 8.0. Each sample was incubated for 40 min at room temperature, diluted 1:2 into denaturing buffer (125 mM Tris, pH 6.8, 4% sodium laurylsulfate, 20% glycerol), and heated to 90 °C for 10 min to denature any noncovalent protein interactions. Each lane of the 4% stacking gel and 7.5 to 17% gradient resolving gel was loaded with 25 μL of the 1:2 sample. The electrophoresis buffer was 25 mM Tris, 192 mM glycine, 0.1% sodium laurylsulfate, pH 8.3. The proteins were visualized with colloidal Coomassie blue stain and the band intensities quantified in an Epi Chemi II Darkroom Gel Documentation System (UVP Labs, Upland, CA). The high molecular weight calibration proteins were from GE Healthcare (Buckinghamshire, UK). The DSS and Coomassie were from Sigma Chemical Co. (St. Louis, MO).

RESULTS

The purpose of this study was to determine the kinetic properties of *S. aureus* primase so that they could be compared to those of other primases, particularly *E. coli*.

Quaternary structure of GST-primase. The quaternary structure of an enzyme must be known before detailed kinetic studies can be designed and/or interpreted. In our previous study, it was shown that the *Schistosoma japonicum* GST tag was required to enhance the solubility of *S. aureus* primase (*14*). Since others have shown that free GST protein is dimeric *in vitro* (*18*) and in crystal form (*19, 20*), it was necessary to determine the fusion protein's quaternary structure. In the presence of reducing agent, 4 μM GST-primase electrophoresed as a monomer at a size of 100 kDa, the predicted size of the fusion protein (Fig. 1, lanes 2). Other workers have reported that GST can undergo oxidative aggregation to form both functional dimers and larger nonfunctional aggregrates (*21*). When the reducing agent was omitted from GST-primase (Fig. 1, lane 1), densitometric scanning showed that 9% of the protein electrophoresed as larger aggregates but none of it as a dimer. Further studies with native gel electrophoresis in the presence of a reducing agent showed that 35 μM GST-primase did not form a heterodimer or larger aggregates when incubated with 150 μM free GST (data not shown). Collectively, these results indicated that the GST tag on primase was not capable of forming oxidized dimers.

The quaternary structure of GST-primase was investigated further by chemical crosslinking in the presence and absence of reducing agent. When 4 μM protein was incubated with 300 μM DSS but no DTT and then subjected to denaturing gel electrophoresis (Fig. 1, lane 3), only 41% of the fusion protein electrophoresed as a

monomer. The remaining 59% were large aggregates that did not migrate into the gel (data not shown). No protein bands were present that would be consistent with dimerization. When GST-primase was incubated with DSS in the presence of a reducing agent, 79% of the material electrophoresed as a monomer and the remainder as higher aggregrates. This property is very different from free GST, 100% of which migrated as dimers after being crosslinked (*22*). Therefore, primase with a GST tag is a stable monomer under reducing conditions but is capable of forming large crosslinked networks under oxidizing conditions. All of the experiments described below are under reducing conditions.

Effect of free GST on GST-primase activity. Free GST was added to the GST-primase to determine whether GST dimerization was capable of affecting the activity of the fusion protein. When 1.5 μM primase and 2 μM ssDNA were incubated in the absence or presence of 1.5 μM free GST, the activity actually rose by 5.8% (the average of duplicate experiments), which was within the normal range of measurement error for these experiments. When 15 μM free GST was added to the reaction, primer synthesis activity was reduced by 12% compared to the absence of GST, indicating weak interference and consistent with a K_i of 110 μM. Therefore, the GST domain of GST-primase does not readily form dimers and does not need to be considered within our working concentration range.

***S. aureus* primase kinetic rate under optimal conditions.** RNA primer synthesis takes place when primase is incubated with magnesium ion, a mixture of four NTPs, and a ssDNA template containing an initiation trinucleotide located 6 nucleotides from the 3'-end (Scheme 1). Primer lengths and amounts were quantified using a denaturing HPLC

assay that is capable of resolving the base and sugar composition of the products (*16*) and analyzed as described in the Materials and Methods. While optimizing the conditions for *S. aureus* primase activity, it was found that the optimal temperature for *in vitro* primer synthesis was 30 °C, with reduced activity at 37 and 15 °C and no detectable activity at 0 or 42 °C (data not shown). Analysis of primase activity at various magnesium concentrations determined that the greatest activity was constant between 10 and 20 mM. There were no RNA primers synthesized in the absence of magnesium and concentrations greater than 20 mM were inhibitory. Primase activity was undetectable in the absence of NTPs, nearly saturated at a NTP concentration of 400 μM, and was maximal at 800 μM. Therefore, 30 °C, 10 mM magnesium ion, and 400 μM NTP concentrations were used for all subsequent experiments.

Under the standard conditions, the primer synthesis catalytic rate was measured in the presence of 2 μM primase and 1 μM ssDNA (Fig. 2). The kinetic data conformed to a single-mode binding saturation relationship $P = P_{app\ max}\ exp(1 - k_{cat}*t)$, where P was the moles of primer synthesized at any given time, $P_{app\ max}$ was the apparent maximum number of primers synthesized, and k_{cat} was the first-order catalytic rate. Nonlinear regression of the data yielded a $P_{app\ max}$ of 48.7 ± 0.5 pmol RNA primers and a k_{cat} of 24.2 (± 0.6) x 10^{-5} s^{-1} and an R^2 of 0.9988. Given that there were 100 pmol template in the reaction, 49% of the templates were primed during the course of the reaction. The was higher than the 25% observed with *E. coli* primase using the d(CTG) template that was also blocked at its 3'-terminus under similar conditions (*16*), indicating that *S. aureus* primase had somewhat higher affinity for its ssDNA template than does *E. coli* primase. The primer synthesis rate for *S. aureus* primase was an order of magnitude slower than

the rate for *E. coli* primase (k_{cat} of 0.00251 s^{-1}) (*9, 16*) and confirms that *de novo* primer synthesis is very slow regardless of the bacterial primase source.

Primase concentration dependence. Given that *S. aureus* primase was monomeric, its activity should be proportional to its concentration. At primase below 400 nM, only primers less than full length were synthesized (Fig. 3A). As the primase concentration was increased to 1.2 μM, all lengths of primers increased and the full-length primers began to grow in. Assuming that primase initiated from the central nucleotide and elongated to the end of the template, the full-length primer would be 16 nucleotides as indicated on the figure. Above 1.2 μM primase, the amount of full-length primers preferentially increased. This pattern of activity suggested that *S. aureus* primase preferentially synthesized primers that were 8 to 10 nucleotides during its first burst of trinucleotide-initiated synthesis, either stalled or dissociated, and then elongated from the short primer's 3'-end until it ran out of template sequence.

When the moles of primer at each length were quantified and then summed to yield total primers synthesized, it was observed that primer synthesis conformed to a hyperbolic relationship with primase concentration (Fig. 3B). This indicated that primase and template were present at limiting concentrations and formed a stoichiometric complex. Since the total concentration of template and primase were known, the data were fit to a quadratic expression that accounted for the maximum fraction of primase-template complex. The fit indicated that 100% of the templates would be primed at saturating primase concentration ($R^2 = 0.985$) and that the apparent dissociation between primase and its ssDNA template was 112 ± 31 nM. This affinity was about 6-fold greater than the affinity between *E. coli* primase and its ssDNA template (*9*).

Primase nucleotide sugar specificity and identification of the initiating nucleotide. In a previous study, *S. aureus* primase primarily initiated RNA primer synthesis complementary to the trinucleotides d(TTA) and d(CTA) (*14*). It had no activity on nineteen other templates including the d(CTG) template that supports *E. coli* primase activity. It was also shown that the *S. aureus* DnaC primase interacted functionally with the *S. aureus* helicase but not with the *E. coli* helicase (*14*). These observations confirmed that the activity observed with the recombinant *S. aureus* proteins were not the result of any contaminating *E. coli* proteins from the *E. coli* overproducing strain.

The presence of a single template guanosine at the antepenultimate position of the d(TTA) template (Scheme 1) was engineered to examine the site-specific insertion properties of the *S. aureus* primase. A series of experiments were performed (Fig. 4) to explore the insertion specificity while at the same time establishing primer lengths and, therefore, the initiating nucleotide. When CTP was omitted from the reaction, *S. aureus* primase generated only one major RNA product (Fig. 4A, lowest chromatogram). This corresponded to the 13-mer RNA species according to our previous study (*16*). When the absorbance scale was increased (data not shown), it was observed that some primers were longer than the 13-mer indicating that some mis-insertion was taking place.

When 400 μM CTP was included in the reaction, the major product was 16-mer RNA plus some 15- and 14-mer RNA (Fig. 4A, second lowest chromatogram). When dCTP was present at 25 or 75 μM, the 13-mer paak decreased while a new peak about one nucleotide longer intensified along. Two other peaks also grew in but with lower intensity. None of these three peaks corresponded with the all-RNA primer elution peaks. In a previous paper, we showed that the missing hydroxyl makes a deoxyribose

more hydrophobic than a ribose so that it interacts more strongly with the alkylated nonporous polystyrene-divinylbenzene copolymer of the reversed phase column (*16*). Therefore, the species that is one nucleotide longer is terminated with a deoxyribonucleoside (dC14 in Fig. 4A) and the two primer species longer than the 14-mer have elongated from the deoxyribolyated terminal sugar. The lower yields of these two elongated primers indicated that primase did so with a lower relative efficiency than from a ribosylated 3'-hydroxyl group.

When ddCTP was present at 25 or 75 μM, *S. aureus* primase, a new peak grew in at a much longer elution time (Fig. 4A, top two chromatograms). The two missing hydroxyls of a terminal ddNMP were much more hydrophobic than a ribo-terminated polymer (*16*) so that it eluted much later than the equivalent ribo-terminated 14-mer. As expected, no products longer than this peak were observed because insertion of a dideoxyribonucleotide causes chain termination. Nevertheless, the ddCTP concentration dependence was similar to that for dCTP, indicating that they are inserted with similar efficiencies and indicating a lack of nucleotide sugar discrimination.

When the chromatogram peaks were quantified and the fraction of primers longer than 14-mers fit to a Michaelis-Menten-like relationship, it was discovered that 5 (± 2)% of the primers in the absence of CTP were the result of mis-insertion at position 14. This was similar to *E. coli* primase in which 6% of RNA primers were longer than 13 nucleotides under nearly indentical conditions (*9*). The fits further indicated that the K_{50} for ddCTP insertion was 27 ± 1 μM (R^2 = 0.9995) and for dCTP insertion plus incorporation was 44 ± 4 μM (R^2 = 0.997). The *S. aureus* enzyme inserts dideoxynucleosides more readily than it inserts deoxynucleosides.

Single-stranded DNA concentration dependence. To determine the stoichiometry or possible sigmoidicity of ssDNA template binding, primer synthesis was measured as a function of CTA template. Below 800 nM template, the predominant product was the full-length 16-mer (Fig. 5A). As the ssDNA was increased, more of the shorter primers were synthesized. The simplest interpretation was that the first functionally bound primase synthesized a short primer of 8-12 nucleotides and then stalled or dissociated. Time and/or more primase were able to prime the remaining templates and to elongate from the initial short primers.

When the moles of primer at each length were quantified and then summed to yield total primers synthesized, it was observed that primer synthesis conformed to a hyperbolic relationship with ssDNA concentration (Fig. 5B). This confirmed that primase and template were present at limiting concentrations and were forming a stoichiometric complex. Since the total concentration of template and primase were known, the data were fit to a quadratic expression that accounted for the maximum fraction of primase-template complex. The fit indicated that 100% of the templates would be primed at saturating ssDNA concentration ($R^2 = 0.993$) and that the apparent dissociation between primase and its ssDNA template was 87 ± 17 nM. This was the same value as determined from the primase titration in Figure 3.

***S. aureus* primase stimulation by replicative helicase.** We have previously shown that *S. aureus* primase was stimulated by its replicative helicase (*14*) but we did not establish the level of helicase stimulation. Therefore, a series of experiments were performed in which a range of *S. aureus* DnaC helicase (up to 500 nM hexamer) was

incubated with *S. aureus* primase at three low concentrations (100, 200 or 400 nM) and 2 μM d(TTA) template.

At 100 nM primase, there was very little primer synthesis in the absence of DnaC helicase (Fig. 6A). As the DnaC concentration increased up to 67 nM hexamer, the amounts of the entire range of primer lengths increased. The areas beneath all primer lengths remained roughly constant as the DnaC was increased up to 250 nM hexamer but then decreased at 500 nM hexamer. Even though the total primer yield was effected by DnaC, the pattern of primer lengths was not. This effect was contrary to the observation that the helicase shortened the primers in the *E. coli* system (*12*).

Similar results were observed with 400 nM primase (Fig. 6B) and 200 nM primase (chromatograms not shown) with the following exceptions: a) there were significant numbers of primers synthesized in the absence of DnaC; b) 500 nM DnaC hexamer did not cause the same degree of inhibition; and c) the DnaC stimulatory effect saturated at higher concentrations as the primase concentration was increased. In fact, maximum stimulation of 200 nM primase occurred between 133 and 250 nM helicase hexamer and maximum stimulation of 400 nM primase occurred between 200 nM and 500 nM. Since 100 nM primase stimulation saturated between 33 and 67 nM, these ratios all suggested that saturation of 2 primases per DnaC hexamer was optimal. The apparent inhibition of 100 nM primase activity by 500 nM DnaC may be due to dilution of the primase monomers bound to the DnaC hexamer or primase-free DnaC hexamers that sequester the ssDNA.

When the moles of primer at each length were quantified and then summed to yield total primers synthesized, it was observed that primer synthesis conformed to a

hyperbolic relationship with regard to DnaC concentration (Fig. 6C). This indicated that the multiple primase monomers were binding independently to the DnaC hexamer. The velocities in the absence and presence of saturating helicase were determined by fitting the data to a saturation relationship (Fig. 6C lines through the data) resulting in a poor fit for the 100 nM primase data (R^2 = 0.53) but with increasingly better fits for the 200 nM (R^2 = 0.82) and 400 nM (R^2 = 0.986) primase data. When the primase activity in the absence of DnaC and in the presence of extrapolated saturating DnaC were plotted versus primase concentration (Fig. 6D), the relationships were roughly linear. This was expected because these reactions were performed with a short incubation time and in the presence of low primase concentration relative to 2 μM d(TTA) template. The ratio of the slopes for primase activity with and without DnaC indicated that the helicase stimulated primase activity by 3.5-fold. This was greater than the stimulation observed in the *G. stearothermophilus* system (*15*) and less than the 15-fold stimulation in the *E. coli* system (*12*).

Effect of helicase on primase initiation specificity. When *E. coli* primase activity was stimulated by its replicative helicase, it initiated from all trinucleotides that were tested (*12, 13*). To determine whether *S. aureus* DnaC also relaxed the initiation specificity of its primase, the d(TTA), d(CTT), d(CTG), or d(TTT) templates (2 μM) were incubated with primase (400 nM) and DnaC (133 nM hexamer) for 30 min (Fig. 7). The d(TTA) template was the only one that supported a significant amount of RNA primer synthesis, just as it was the best template for primase when it acted alone. Therefore, *S. aureus* DnaC helicase did not relax the initiation specificity of *S. aureus* primase.

DISCUSSION

The observations made in this study suggest that most but not all properties of the eubacterial primase protein are conserved. The findings complement the growing amount of structural and functional data for this important class of proteins.

Functional similarities related to mechanism and substrate specificity. The *S. aureus* and *E. coli* enzymes are most similar during the initiation phase of their mechanisms. Both enzymes initiated from the central nucleotide of a specific trinucleotide sequence within the template. They differ in that *S. aureus* primase initiates primer synthesis primarily from d(TTA) and d(CTA) (*14*) while *E. coli* primase initiates from d(CTG) (*13, 23*). Both enzymes form the first phosphodiester bond very slowly and the next 8-10 bonds much more quickly. At this point, the enzyme either becomes less processive or dissociates. The structurally divergent eukaryotic/archaeal primases (*6, 24, 25*) share these initiation features even though they do not initiate from specific trinucleotides (*26*). Therefore, primases are inherently slow but produce polymers of discrete lengths regardless of the primase source.

A recent macroscopic kinetic model from the Viljoen lab predicts that sampling the dNTP pool is a critical factor in determining the elongation rate of DNA polymerases (*27*). At each step along the DNA template, the polymerase withdraws dNTPs from the pool until it finds the complementary nucleotide and only then will it begin catalysis. As an analogy to that model, we propose that primer synthesis initiation is slow because primase samples both the ssDNA sequence and the available NTP pool until a preferred initiating trinucleotide is assembled with two complementary NTPs. Considering that primase crystal structures from both the Berger and Kuriyan labs show that the active site

is very exposed (*28, 29*), it is reasonable to expect that the complex between the initiation trinucleotide and its two complementary NTPs will not be stable until the N-terminal zinc-binding domain (ZBD) clamps onto it.

The *S. aureus* and *E. coli* primases are also similar in their low discrimination against the insertion of NTPs, dNTPs, or ddNTPs. This lack of sugar insertion specificity is shared with eukaryotic primases (*30*), again indicating an inherent primase function that is most likely the result of convergent structural features. Similarly, both bacterial primases elongate much slower from a terminal dNMP than from an NMP. For both enzymes, insertion of a dNMP may provide a signal to the DNA polymerase to take over.

Primase is a functional monomer *in vitro*. There is evidence in the literature that primase dimerizes. For instance, *E. coli* primase binds to G4 origin-containing ssDNA as a dimer according to both crosslinking and electrophoretic mobility shift experiments with support from solution binding studies (*10*). G4ori DNA is very different from the unstructured ssDNA used in the current study however. The G4 ori DNA forms hairpins, is able to bind ssDNA binding protein in a special way, and most importantly is able to bind two primases (*9, 11, 23, 31, 32*). The ssDNA templates used in this study are incapable of forming these special stable hairpins. In another study using fluorescence resonance transfer, the ZBD of one *Aquifex aeolicus* primase monomer was able to bind near the active site of another monomer in the presence of ssDNA (*33*). These experiments were performed at room temperature where this thermophilic primase must bind particularly strongly to the ssDNA. When these observations are added to the hypothesis that the fork helicase stimulates primer synthesis by serving as a platform

upon which two or more primases assemble so that they can interact (*15, 34*), it raises the question whether primase is a functional monomer or dimer when it acts alone.

In the current study with *S. aureus* primase, the hyperbolic primase-dependence of synthesis indicates that primase functions as a monomer *in vitro*. Primase could not be crosslinked to form dimers and our numerous attempts to photocrosslink primase and ssDNA using either UV-irradiation of ^{32}P-end labeled ssDNA or iodated uracil-containing ssDNA showed only monomeric primase-ssDNA complexes (data not shown). Therefore, the interaction between primase and ssDNA is weak and transient such that fork helicase and/or auxiliary proteins are probably required to bring multiple monomers in proximity with one another.

Functional differences relate to helicase stimulation. The major functional differences between *S. aureus* and *E. coli* primases relate to their interactions with their respective replicative helicases. In the *S. aureus* system, DnaC helicase stimulates primase activity 3.5-fold, does not alter the primase initiation specificity, and does not alter the pattern of primers synthesized by very much. The *E. coli* DnaB helicase stimulates its primase by 15-fold, broadens the primase initiation specificity to all trinucleotide sequences, and limits the RNA primer size to 12 bases or less (*12, 13*).

The different interactions that we have reported for the primase-helicase interaction between Gram-negative *E. coli* and Gram-positive *S. aureus* may reflect the different structures of the primase C-terminal domain (CTD) (*35, 36*). Specifically, the CTD from Gram-negative *E. coli* primase has a long helix 5 that holds its extreme C-terminal helix-turn-helix helicase-interacting subdomain far from the 5-helix bundle that makes up its other subdomain. This differs with Gram-positive *G. stearothermophilus* primase CTD,

which has two bends in its equivalent to the *E. coli* helix 5 so that its extreme C-terminal helix-turn-helix clusters with the 5-helix bundle.

ACKNOWLEDGMENTS

This work was supported in part by a grant from the Department of Defense, Defense Advanced Research Program Agency (award W911NF0510275).

FIGURE CAPTIONS AND FIGURES

FIG. 1. Crosslinking of GST-Primase as analyzed by denaturing gel electrophoresis. Primase (4 μM) was incubated in the absence or presence of reducing agent and/or crosslinking agent. The sizes of the molecular weight markers are indicated. The GST-primase monomer mass is 101.7 kDa based on its sequence. The GST-primase monomer mass is 100.4 kDa as calculated from a comparison to the standards on this gel.

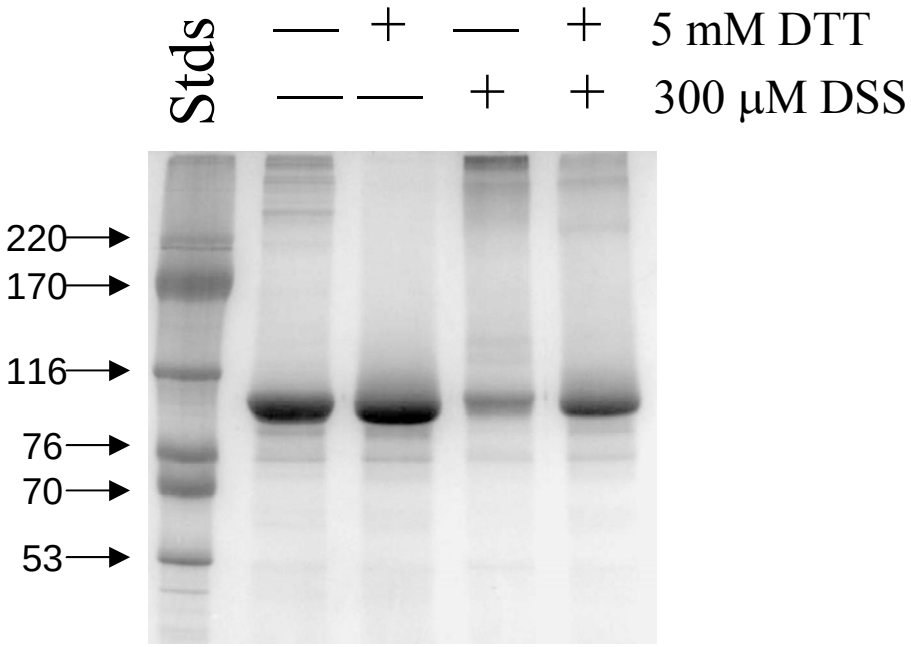

FIG. 2. Primer synthesis time course was visualized by denaturing HPLC (left) and quantified (right). The d(TTA) template was 1 μM, the primase was 2 μM, and the samples were incubated for 30, 60, 120 and 180 min. Each sample was gathered in triplicate but only one representative chromatogram was reproduced below. In the figure to the right, the average and standard deviation of three experiments were plotted even though the size of the circles was sometimes larger than the standard deviation. The line through the quantified data conformed to the first-order rate equation.

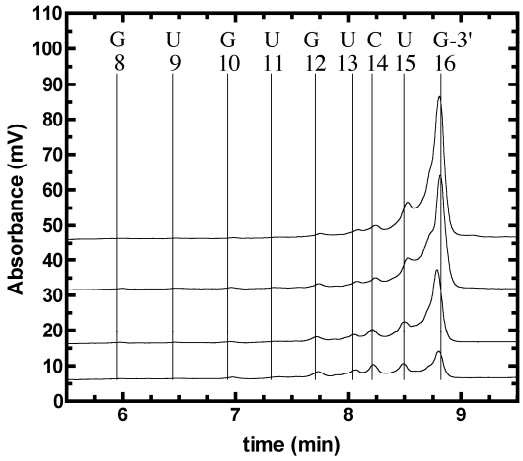

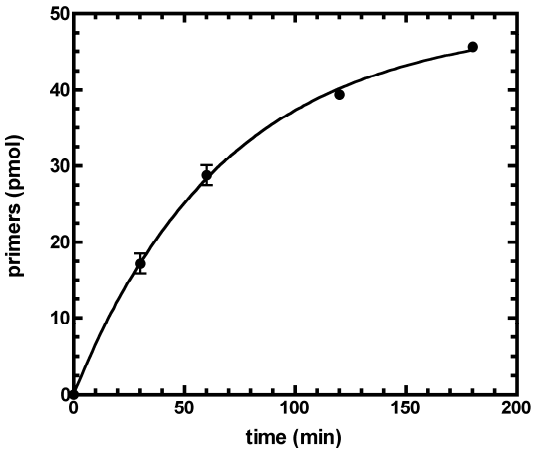

FIG. 3. Primase-concentration dependence of RNA primer synthesis was visualized by denaturing HPLC (left) and quantified (right). The d(CTA) template concentration was 2 μM, the primase concentrations are indicated on the chromatograms, and all samples were incubated for 90 min. The dashed line indicates the theoretical stoichiometric case in which 1 primer would be synthesized per template. The solid line through the quantified data conformed to the quadratic equation for primase-ssDNA complex formation from its components.

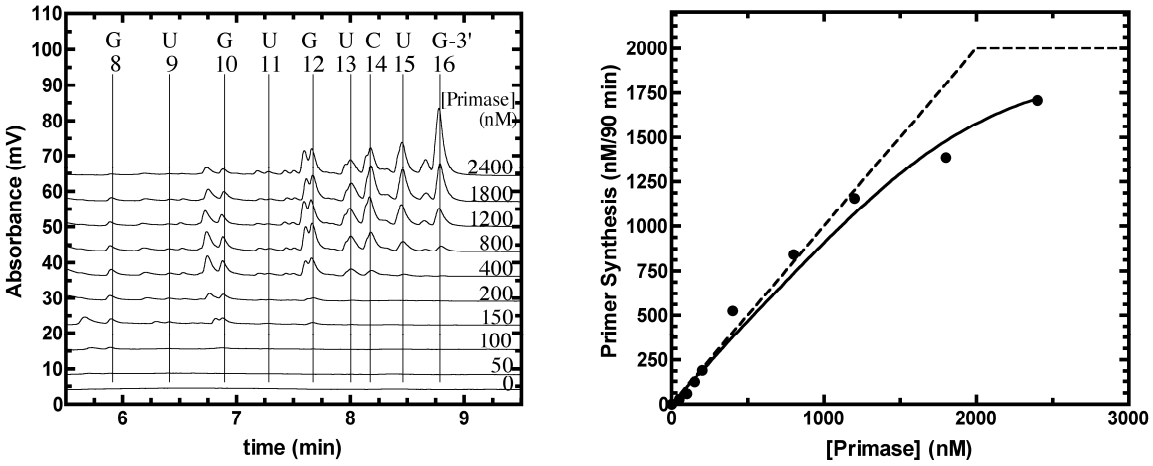

FIG. 4. Site-specific nucleotide insertion was visualized by denaturing HPLC (left) and quantified (right). In all reactions, the d(CTA) template concentration was 1.5 μM, the primase concentration was 1.5 μM, all samples were incubated for 60 min, and 400μM each of ATP, UTP and GTP were present. There was no CTP in any of the samples. The d(CTA) template (in fact, all templates) had a guanine in the antepenultimate position so that primase would only be able to synthesize a 14-mer that initiated from the trinucleotide's thymine in the presence of CTP or suitable substitutes. In the chromatograms from bottom to top, the samples contained: no CTP, 400 μM CTP; 25 μM dCTP; 75 μM dCTP; 25 μM ddCTP; and 75 μM ddCTP. The solid line through the quantified data in panel B conformed to a modified Michaelis-Menten relationship that allowed for a minimum fraction of mis-insertion and/or mis-incorporation.

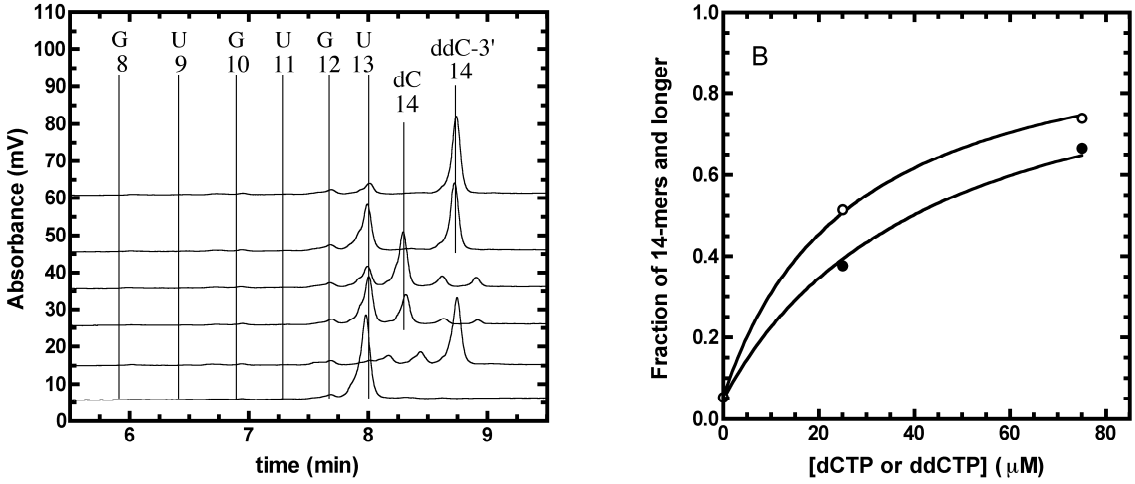

FIG. 5. Template-concentration dependence of RNA primer synthesis was visualized by denaturing HPLC (left) and quantified (right). The d(CTA) template concentration are indicated on the chromatograms, the primase concentration was 2 μM, and all samples were incubated for 90 min. The dashed line indicates the theoretical stoichiometric case in which 1 primer would be synthesized per template. The solid line through the quantified data conformed to the quadratic equation for primase-ssDNA complex formation from its components.

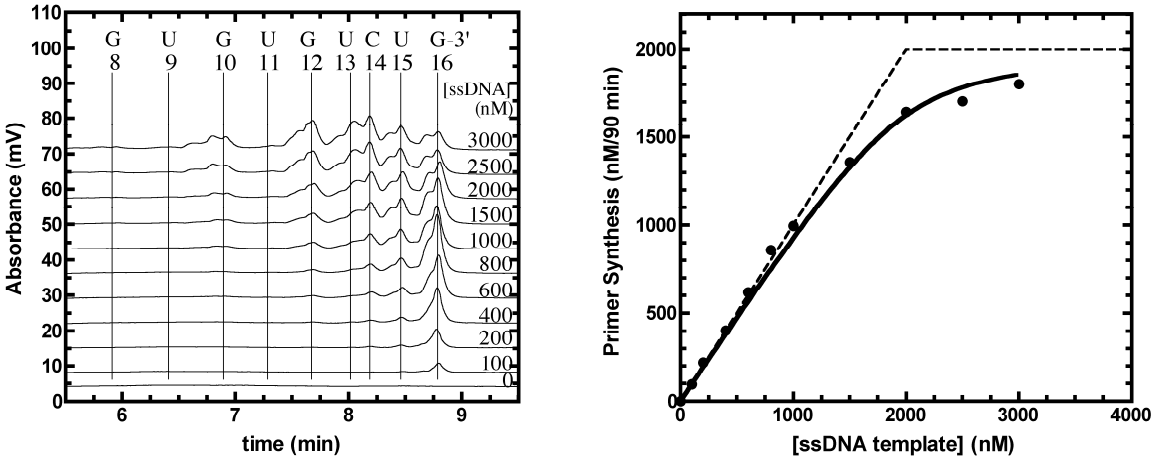

FIG. 6. Helicase stimulation of RNA primer synthesis was visualized by denaturing HPLC (A shows 100 nM primase, 200 nM primase chromatograms are not shown, and B shows 400 nM primase). The concentrations of *S. aureus* DnaC helicase hexamer are indicated on the chromatograms. The d(TTA) template concentration was 2 μM and all samples were incubated for 30 min. The lowest chromatogram in A was a negative control containing buffer but no enzymes or ssDNA. After the primer yields were calculated, *S. aureus* primase activity was plotted versus *S. aureus* DnaC helicase concentration and fit to the relevant saturation equation (C). Then, the primase activity in the absence (D, open circles) and extrapolated maximal activity in the presence of helicase (D, filled circles) were plotted versus primase concentration.

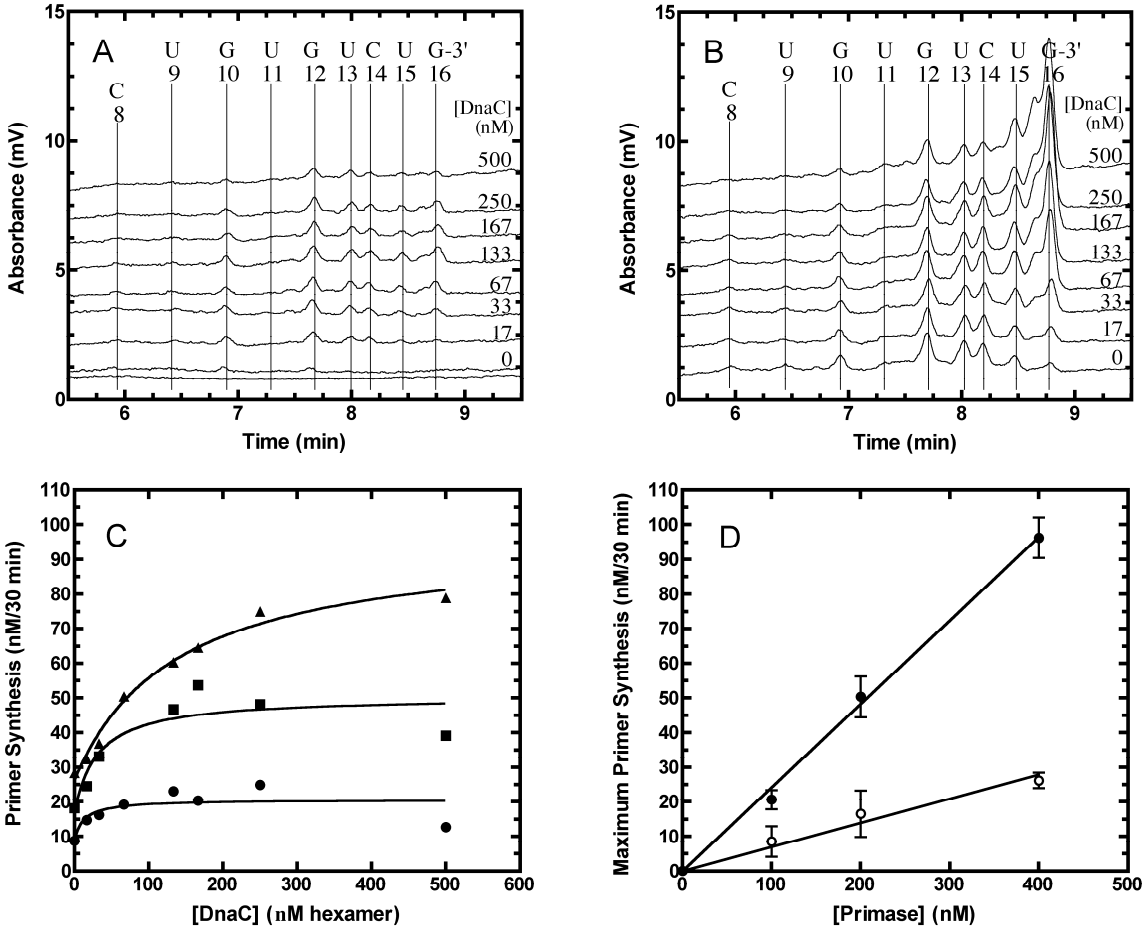
A
B
C
D
U 9
G 10
U 11
G 12
U 13
C 14
U 15
G-3' 16
C 8
[DnaC] (nM)
500
250
167
133
67
33
17
0
Absorbance (mV)
Time (min)
Primer Synthesis (nM/30 min)
[DnaC] (nM hexamer)
Maximum Primer Synthesis (nM/30 min)
[Primase] (nM)

FIG. 7. Primase initiation specificity when stimulated by helicase was visualized by denaturing HPLC. The primase concentration was 400 nM, the DnaC hexamer concentration was 133 nM, and all samples were incubated for 30 min. The template concentration was 2 μM and had the sequence 5'-CAGA$(CA)_5$XYZ$(CA)_3$-3', where XYZ is the initiation trinucleotide indicated on the chromatograms.

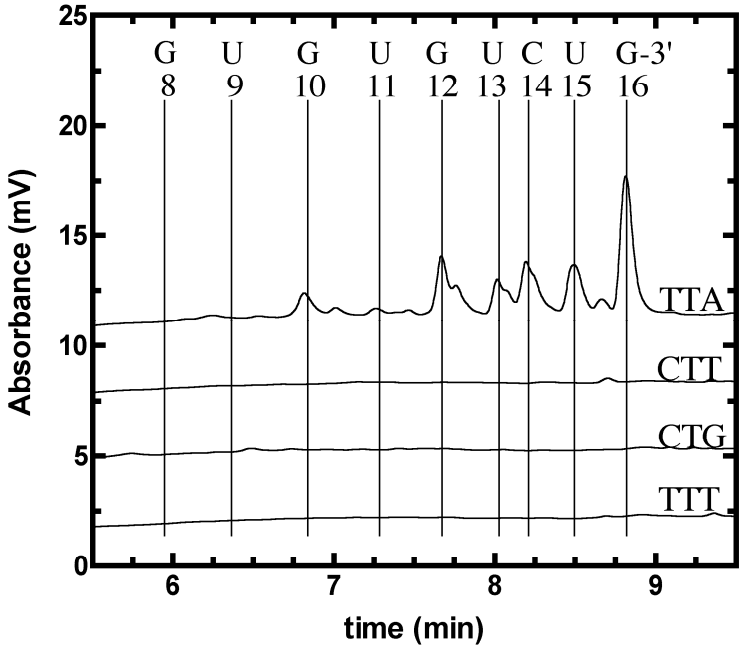

SCHEME TITLE AND SCHEME

SCHEME 1. *S. aureus* primase activity assay using the d(TTA) template.

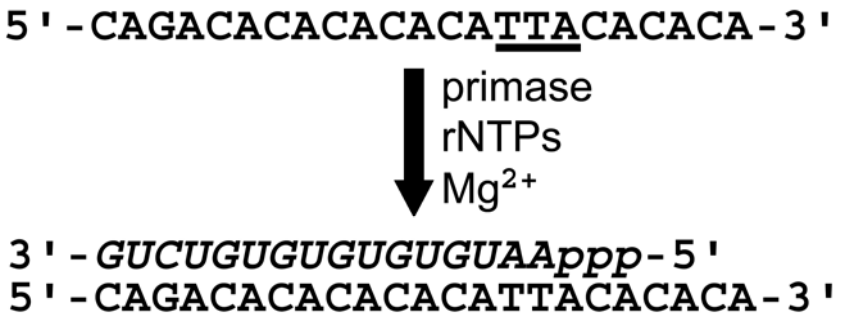

TABLES

TABLE 1. Single-stranded DNA templates

Name	5'-3' Sequence[a]	ε ($M^{-1}cm^{-1}$)
d(CTA) template	d(CAGACACACACACACTACACACA)	229,600
d(CTG) template	d(CAGACACACACACACTGCACACA)	225,500
d(CTT) template	d(CAGACACACACACACTTCACACA)	224,700
d(GTA) template	d(CAGACACACACACAGTACACACA)	234,100
d(TTA) template	d(CAGACACACACACATTACACACA)	231,500
d(TTT) template	d(CAGACACACACACATTTCACACA)	226,600

[a] The 3'-hydroxyl of all templates is blocked with C3 propanediol.

TABLE 2. Molar Extinction Coefficients of Various RNA Polymers[a]

Length	ε ($M^{-1}cm^{-1}$)	RNA Sequence	Relative Extinction
16	144,000	AGUGUGUGUGUGUCUG	(1.000)
15	135,000	AGUGUGUGUGUGUCU	0.938
14	127,200	AGUGUGUGUGUGUC	0.883
13	121,000	AGUGUGUGUGUGU	0.840
12	112,500	AGUGUGUGUGUG	0.781
11	103,500	AGUGUGUGUGU	0.719
10	95,000	AGUGUGUGUG	0.660
9	86,000	AGUGUGUGU	0.597
8	77,500	AGUGUGUG	0.538

[a]The extinction coefficients were calculated with IDT OligoAnalyzer 3.0 by the nearest neighbor method using accurate nucleotide extinction coefficients (*37*).

References

1. Griep, M. A. (2001) Primase, in *Encyclopedia of Genetics* (Brenner, S., and Miller, J., Eds.), Academic Press, New York.
2. Frick, D. N., and Richardson, C. C. (2001) DNA primases, *Annu. Rev. Biochem. 70*, 39-80.
3. Grompe, M., Versalovic, J., Koeuth, T., and Lupski, J. R. (1991) Mutations in the *Escherichia coli dnaG* gene suggest coupling between DNA replication and chromosome partitioning, *J. Bacteriol. 173*, 1268-1278.
4. Liu, J., Dehbi, M., Moeck, G., Arhin, F., Bauda, P., Bergeron, D., Callejo, M., Ferretti, V., Ha, N., Kwan, T., McCarty, J., Srikumar, R., Williams, D., Wu, J. J., Gros, P., Pelletier, J., and DuBow, M. (2004) Antimicrobial drug discovery through bacteriophage genomics, *Nat. Biotechnol. 22*, 185-191.
5. Augustin, M. A., Huber, R., and Kaiser, J. T. (2001) Crystal structure of a DNA-dependent RNA polymerase (DNA primase), *Nat. Struct. Biol. 8*, 57-61.
6. Keck, J. L., and Berger, J. M. (2001) *Primus inter pares* (first among equals), *Nat. Struct. Biol. 8*, 2-4.
7. Zhang, Y., Yang, F. D., Kao, Y. C., Kurilla, M. G., Pompliano, D. L., and Dicker, I. B. (2002) Homogenous assays for *Escherichia coli* DnaB-stimulated DnaG primase and DnaB helicase and their use in screening for chemical inhibitors, *Anal. Biochem. 304*, 174-179.
8. Hegde, V. R., Pu, H., Patel, M., Black, T., Soriano, A., Zhao, W., Gullo, V. P., and Chan, T.-M. (2004) Two new bacterial DNA primase inhibitors from the plant *Polygonum cuspidatum*, *Bioorg. Med. Chem. Lett. 14*, 2275-2277.

9. Swart, J. R., and Griep, M. A. (1995) Primer synthesis kinetics by *Escherichia coli* primase on single-stranded DNA templates, *Biochemistry 34*, 16097-16106.

10. Khopde, S., Biswas, E. E., and Biswas, S. B. (2002) Affinity and sequence specificity of DNA binding and site selection for primer synthesis by *Escherichia coli* primase, *Biochemistry 41*, 14820-14830.

11. Stayton, M. M., and Kornberg, A. (1983) Complexes of *Escherichia coli* primase with the replication origin of G4 phage DNA, *J. Biol. Chem. 258*, 13205-13212.

12. Johnson, S. K., Bhattacharyya, S., and Griep, M. A. (2000) DnaB helicase stimulates primer synthesis activity on short oligonucleotide templates, *Biochemistry 39*, 736-744.

13. Bhattacharyya, S., and Griep, M. A. (2000) DnaB helicase affects the initiation specificity of *Escherichia coli* primase on single-stranded DNA templates, *Biochemistry 39*, 745-752.

14. Koepsell, S. A., Larson, M. A., Griep, M. A., and Hinrichs, S. H. (2006) *Staphylococcus aureus* Helicase but Not *Escherichia coli* Helicase Stimulates *S. aureus* Primase Activity and Maintains Initiation Specificity, *J. Bacteriol. 188*, 4673-4680.

15. Thirlway, J., and Soultanas, P. (2006) In the *Bacillus stearothermophilus* DnaB-DnaG complex, the activities of the two proteins are modulated by distinct but overlapping networks of residues, *J. Bacteriol. 188*, 1534-1539.

16. Koepsell, S., Bastola, D., Hinrichs, S. H., and Griep, M. A. (2004) Thermally-denaturing HPLC analysis of primase activity, *Anal. Biochem. 332*, 330-336.

17. Hames, B. D., and Rickwood, D. (1990) *Gel Electrophoresis of Proteins: A Practical Approach*, 2nd ed., IRL Press, Oxford.

18. Walker, J., Crowley, P., Moreman, A. D., and Barrett, J. (1993) Biochemical properties of cloned glutathione S-transferases from *Schistosoma mansoni* and *Schistosoma japonicum*, *Mol Biochem Parasitol 61*, 255-264.

19. Lim, K., Ho, J. X., Keeling, K., Gilliland, G. L., Ji, X., Ruker, F., and Carter, D. C. (1994) Three-dimensional structure of *Schistosoma japonicum* glutathione S-transferase fused with a six-amino acid conserved neutralizing epitope of gp41 from HIV, *Protein Sci. 3*, 2233-2244.

20. McTigue, M. A., Williams, D. R., and Tainer, J. A. (1995) Crystal structures of a schistosomal drug and vaccine target: glutathione S-transferase from *Schistosoma japonica* and its complex with the leading antischistosomal drug praziquantel, *J. Mol. Biol. 246*, 21-27.

21. Kaplan, W., Husler, P., Klump, H., Erhardt, J., Sluis-Cremer, N., and Dirr, H. (1997) Conformational stability of pGEX-expressed *Schistosoma japonicum* glutathione S-transferase: a detoxification enzyme and fusion-protein affinity tag, *Protein Sci. 6*, 399-406.

22. Tudyka, T., and Skerra, A. (1997) Glutathione S-transferase can be used as a C-terminal, enzymatically active dimerization module for a recombinant protease inhibitor, and functionally secreted into the periplasm of *Escherichia coli*, *Protein Sci. 6*, 2180-2187.

23. Swart, J. R., and Griep, M. A. (1993) Primase from *Escherichia coli* primes single-stranded templates in the absence of single-stranded DNA-binding protein

or other auxiliary proteins: Template sequence requirements based on the bacteriophage-G4 complementary strand origin and Okazaki fragment initiation sites, *J. Biol. Chem. 268*, 12970-12976.

24. Ito, N., Nureki, O., Shirouzu, M., Yokoyama, S., and Hanaoka, F. (2003) Crystal structure of the *Pyrococcus horikoshii* DNA primase-UTP complex: Implications for the mechanism of primer synthesis, *Genes to Cells 8*, 913-923.

25. Ito, N., Nureki, O., Shirouzu, M., Yokoyama, S., and Hanaoka, F. (2001) Crystallization and preliminary X-ray analysis of a DNA primase from hyperthermophilic archaeon *Pyrococcus horikoshii*, *J. Biochem. 130*, 727-730.

26. Sheaff, R. J., and Kuchta, R. D. (1993) Mechanism of calf thymus DNA primase - slow initiation, rapid polymerization, and intelligent termination, *Biochemistry 32*, 3027-3037.

27. Viljoen, S., Griep, M. A., Nelson, M., and Viljoen, H. (2005) A macroscopic kinetic model for DNA polymerase elongation and high-fidelity nucleotide selection, *Comp. Biol. Chem. 29*, 101-110.

28. Keck, J. L., Roche, D. D., Lynch, A. S., and Berger, J. M. (2000) Structure of the RNA polymerase domain of *E. coli* primase, *Science 287*, 2482-2486.

29. Podobnik, M., McInerney, P., O'Donnell, M., and Kuriyan, J. (2000) A TOPRIM domain in the crystal structure of the catalytic core of *Escherichia coli* primase confirms a structural link to DNA topoisomerases, *J. Mol. Biol. 300*, 353-362.

30. Sheaff, R. J., and Kuchta, R. D. (1994) Misincorporation of nucleotides by calf thymus DNA primase and elongation of primers containing multiple noncognate nucleotides by DNA-polymerase-alpha, *J. Biol. Chem. 269*, 19225-19231.

31. Sun, W. L., and Godson, G. N. (1993) Binding and phasing of *Escherichia coli* single-stranded DNA-binding protein by the secondary structure of phage-G4 origin of complementary-DNA strand synthesis (G4oriC), *J. Biol. Chem. 268*, 8026-8039.

32. Sun, W. L., and Godson, G. N. (1996) Interaction of *Escherichia coli* primase with a phage G4ori(c)-*E. coli* SSB complex, *J. Bacteriol. 178*, 6701-6705.

33. Corn, J. E., Pease, P. J., Hura, G. L., and Berger, J. M. (2005) Crosstalk between primase subunits can act to regulate primer synthesis in trans, *Mol. Cell 20*, 391-401.

34. Corn, J. E., and Berger, J. M. (2006) Regulation of bacterial priming and daughter strand synthesis through helicase-primase interactions, *Nuc. Acids Res. 34*, 4082-4088.

35. Oakley, A. J., Loscha, K. V., Schaeffer, P. M., Liepinsh, E., Pintacuda, G., Wilce, M. C., Otting, G., and Dixon, N. E. (2005) Crystal and solution structures of the helicase-binding domain of *Escherichia coli* primase, *J. Biol. Chem. 280*, 11495-11504.

36. Syson, K., Thirlway, J., Hounslow, A. M., Soultanas, P., and Waltho, J. P. (2005) Solution structure of the helicase-interaction domain of the primase DnaG: A model for helicase activation, *Structure 13*, 609-616.

37. Cavaluzzi, M. J., and Borer, P. N. (2004) Revised UV extinction coefficients for nucleoside-5'-monophosphates and unpaired DNA and RNA, *Nuc. Acids Res. 32*, e13.

Available online at www.sciencedirect.com
ScienceDirect
Bioorganic & Medicinal Chemistry
ELSEVIER
Bioorganic & Medicinal Chemistry xxx (2007) xxx–xxx

Myricetin inhibits *Escherichia coli* DnaB helicase but not primase

Mark A. Griep,[a,c,*] Sheldon Blood,[a] Marilynn A. Larson,[b,c] Scott A. Koepsell[b,c] and Steven H. Hinrichs[b,c]

[a]*Department of Chemistry, University of Nebraska-Lincoln, 614 Hamilton Hall, Lincoln, NE 68588-0304, USA*
[b]*Department of Microbiology and Pathology, University of Nebraska Medical Center, Omaha, NE 68198, USA*
[c]*Nebraska Center for Biosecurity, University of Nebraska Medical Center, Omaha, NE 68198, USA*

Received 3 April 2007; revised 29 June 2007; accepted 3 July 2007

Abstract—Primase and DnaB helicase play central roles during DNA replication initiation and elongation. Both enzymes are drug targets because they are essential, persistent among bacterial genomes, and have different sequences than their eukaryotic equivalents. Myricetin is a ubiquitous natural product in plants that is known to inhibit a variety of DNA polymerases, RNA polymerases, reverse transcriptases, and telomerases in addition being able to inhibit kinases and helicases. We have shown that myricetin inhibits *Escherichia coli* DnaB helicase according to a mechanism dominated by noncompetitive behavior with a K_i of 10.0 ± 0.5 μM. At physiological ATP concentration, myricetin inhibits *E. coli* DnaB helicase with an inhibitory concentration at 50% maximal (IC_{50}) of 11.3 ± 1.6 μM. In contrast, myricetin inhibited *E. coli* primase at least 60-fold weaker than DnaB helicase and far weaker than any other polymerase.

1. Introduction

Helicase and primase are required during DNA replication because DNA is an antiparallel duplex and because no replicative DNA polymerase is able to initiate polymers de novo. Primase is a specialized DNA-dependent RNA polymerase that generates short oligoribonucleotide polymers de novo that can be elongated by DNA polymerase.[1,2] During DNA replication, primase initiates the leading strand synthesis at least once and the lagging strand synthesis many times. Even though all autonomous life forms store their genetic information in duplex DNA and use a primase to initiate leading and lagging strand DNA synthesis, the primases from archaea and eukaryotes are structurally unrelated to the primases from prokaryotes.[3,4] In *Escherichia coli*, conditionally lethal mutations in the primase gene yield lethal phenotypes under the non-permissive conditions, demonstrating the essentiality of the enzyme.[5,6] The indispensable function of primase and the structural divergence of the eukaryotic and prokaryotic primases have led to the identification of the enzyme as a target for novel antibiotic development.[7,8]

The DnaG protein from *E. coli* is the model eubacterial primase because its structure and function have been extensively characterized. It has been demonstrated that *E. coli* DnaG primase is slow, binds ssDNA as a dimer, and that interaction with DnaB helicase stimulates its catalytic activity over 15-fold.[9–12] *E. coli* DnaG primase specifically initiates RNA primer synthesis complementary to the trinucleotide 5′-d(CTG)-3′ in vitro, and *E. coli* Okazaki fragment initiation maps to a d(CTG) on the chromosomal template strand in vivo.[13,14]

DnaB helicase from *E. coli* is the model eubacterial helicase that unwinds duplex DNA at the replication fork so that the two strands can be replicated by the combination of primase and DNA polymerase.[15] In *E. coli*, conditionally lethal mutations in the *dnaB* gene yielded lethal phenotypes under the non-permissive conditions, demonstrating the essentiality of the gene product for replication elongation and initiation.[16–20] During the initiation phase of replication, *E. coli* DnaB helicase interacts with DnaA origin-binding protein, DnaC helicase loading protein, and primase.[21,22] During the elongation phase, dimeric DNA polymerase III is tethered to the helicase via its tau subunit and primase repeatedly

Abbreviation: ssDNA, single-stranded DNA.
Keywords: Myricetin; DNA replication; DnaB helicase; Primase; *Escherichia coli*.
* Corresponding author. Tel.: +1 402 472 3429; fax: +1 402 472 9402; e-mail: mgriep1@unl.edu

0968-0896/$ - see front matter © 2007 Published by Elsevier Ltd.
doi:10.1016/j.bmc.2007.07.057

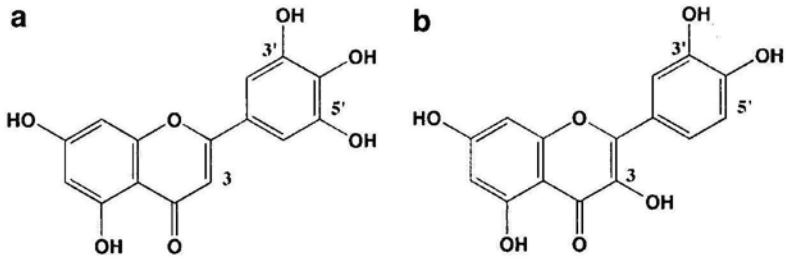

Figure 1. The structures of (a) myricetin and (b) quercetin differ with regard to the hydroxyls on carbons 3 and 5′. Tests with a variety of flavonoids revealed that the 3′ and 5′ hydroxyls of myricetin were very important for its ability to inhibit RSF1010 RepA helicase better than the other flavonoids.[57]

and transiently interacts with the helicase to initiate lagging strand synthesis.[23,24] During the termination phase, the replication machinery is prevented from over-replicating the genome by the inhibitory interaction between the Tus protein and DnaB helicase.[25] As the central hub of the replication machinery and given the structural divergence of the eukaryotic and prokaryotic fork helicases, DnaB is considered to be a novel target for antibiotic development.

High-throughput assays have been developed for helicase activity, primase activity, and helicase-stimulated primase activity to identify novel inhibitors of these two enzymes.[26,27,7,28] Primase activity assays have been used to identify several natural product inhibitors, such as a bicyclic macrolide, two phenolic saccharides, and a group of synthetic compounds identified from a series of virtual and real screens.[29,8,30] The phenolic saccharides are not good leads because they inhibit primase activity through their ability to bind to ssDNA and thereby occlude primase. Helicase activity assays have identified inhibitors from among the known families of flavonols and triaminotriazines.[31,32] These families of compounds inhibit many helicases and/or kinases.[31–33]

Flavonoids provide flavor and color to all parts of plants. Over 5000 different flavonoids, including myricetin and quercetin (Fig. 1), have been described and some of them have been tested for biological activity.[34] Many flavonoids have anti-carcinogenic and antibacterial activities but the sites of action are known for only a few.[35] One of the exceptions is that quercetin's antimicrobial activity can be attributed in part to its inhibition of gyrase. Myricetin has been shown to have antimicrobial activity but it has not been possible to attribute its effect to any one target. Determining its target has been difficult because flavonoids tend to aggregate, adhere to the container surface, and immobilize the enzyme being assayed so that it is inactivated by a nondrug-like mechanism.[36,37] Nevertheless, careful analysis has shown that myricetin and quercetin inhibit a variety of DNA polymerases, RNA polymerases, reverse transcriptases, and telomerases.[38–41]

In the present study, it was discovered that DnaB helicase activity was 60 times more sensitive to myricetin than was primase activity. In fact, primase was the least myricetin-sensitive of all polymerases tested so far. The myricetin inhibition kinetics of the DnaB ATPase activity were consistent with simple noncompetitive inhibition with physiological amounts of the substrate ATP.

2. Results

The purpose of this study was to determine the extent to which myricetin was capable of inhibiting *E. coli* DnaB helicase, primase, and DnaB-stimulated primase activity. The results showed that DnaB helicase was much more sensitive to myricetin than was primase.

2.1. Myricetin inhibition of DnaB ATPase activity

After some preliminary experiments to establish the best range of concentrations, the inhibition of DnaB ATPase activity was analyzed as a function of ATP and myricetin. In the absence of myricetin (Fig. 2a and b), the ATP concentration dependence exhibited hyperbolic saturation kinetics with a K_M of 31 μM ATP and V_{max} = 2870 nM/s (Table 1). These were similar to reported values.[42,43] Hyperbolic kinetics indicated that all of the ATP active sites were equal and non-interacting even though the enzyme has six identical subunits per functional complex. As the myricetin was increased to 12 μM, the apparent V_{max} decreased 2.7-fold whereas the apparent K_M decreased 11-fold. The decrease in the apparent K_M was not consistent with competition between ATP and myricetin for the active site. Simple competitive inhibition would have increased the K_M according to the relationship of $K'_M = K_M(1 + [I]/K_i)$, where K'_M is the apparent K_M and K_i is the median inhibition concentration. When myricetin was increased to 30 μM, the apparent K_M and apparent V_{max} decreased by about the same amount indicating that the kinetic affinity for ATP was no longer being so dramatically affected. Higher myricetin concentration led to a continued decrease in apparent V_{max} but an increase in the apparent K_M, which was finally consistent with some small degree of competitive inhibition.

The decrease in apparent V_{max} suggested that it may be due to noncompetitive inhibition, in which the inhibitor is able to bind to both the free enzyme and the enzyme–substrate complex to create a "dead end" complex that is inactive. Simple noncompetitive inhibition decreases the V_{max} according to the relationship of $V'_{max} = V_{max}/(1 + [I]/K_i)$, where V'_{max} is the apparent V_{max} and K_i is the median inhibition concentration. The

Please cite this article in press as: Griep, M. A. et al., *Bioorg. Med. Chem.* (2007), doi:10.1016/j.bmc.2007.07.057

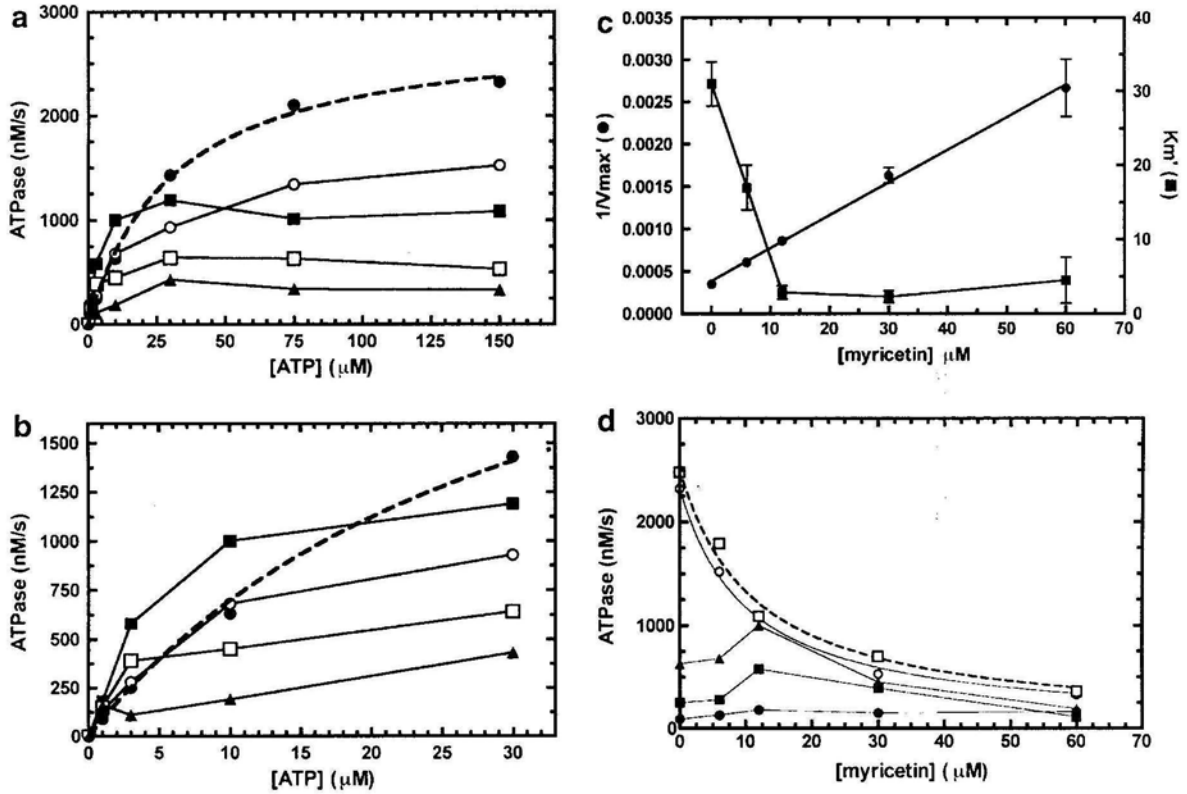

Figure 2. The effect of ATP and myricetin on *E. coli* DnaB ATPase. In panels a and b, the myricetin concentrations were 0 μM (●), 12 (■), 30 (□), and 60 (▲). In panel c, apparent kinetic constants from the data were plotted versus myricetin concentration. In panel d, the ATPase activity was replotted versus myricetin concentration such that the ATP concentrations were 1 μM (●), 3 μM (■), 10 μM (▲), 150 μM (○), and 1 mM ATP (□).

Table 1. Apparent Michaelis–Menten constants for *E. coli* DnaB helicase in the presence of myricetin

Myricetin (μM)	V'_{max} (μM/s)	K'_M (μM)	R^2
0	2.87 ± 0.09	31 ± 3	0.998
6	1.64 ± 0.08	17 ± 3	0.989
12	1.06 ± 0.07	2.9 ± 0.9	0.958
30	0.61 ± 0.04	2.3 ± 0.8	0.952
60	0.35 ± 0.05	4.5 ± 3.1	0.801

mathematical inversion of this equation ($1/V'_{max} = 1/V_{max} + [I]/V_{max}K_i$) indicates that a plot of $1/V'_{max}$ versus [I] will be linear if it conforms to noncompetitive inhibition and that the slope and *y*-intercept can be used to determine the inhibition constant. When the data were so plotted, they yielded a linear relationship (Fig. 2c circles) and a K_i of 10.0 ± 0.5 μM. Therefore, the decrease in enzyme activity as a function of myricetin at saturating ATP was due to noncompetitive inhibition.

To determine the inhibitor concentration that causes 50% inhibition, IC_{50}, the ATPase activity was replotted versus myricetin concentration (Fig. 2d). At the highest ATP concentrations, 150 μM (solid line) and 1 mM (dashed line), the data conformed to the inhibition equation: % activity = $Y_{max} - Y_{max}$ [I]/(IC_{50} + [I]). Fitting the 150 μM ATP data revealed that the Y_{max} was 2340 ± 50 nM/s and IC_{50} was 10.2 ± 0.6 μM myricetin with an R^2 of 0.997. At 1 mM ATP, the Y_{max} was 2510 ± 110 nM/s and IC_{50} was 11.3 ± 1.6 μM myricetin with an R^2 of 0.986. These values were statistically the same as the K_i, showing that the dominant inhibition mechanism at high and saturating ATP was noncompetitive. An examination of the myricetin effect (Fig. 2d) further showed that myricetin stimulated ATPase when its concentration was less than 12 μM and the ATP concentration was less than 10 μM. At these low non-physiological ATP concentrations (Fig. 2d), the K_M effects (Fig. 2c) indicate that myricetin binding to non-active sites was able to enhance ATPase activity by increasing the enzyme's kinetic affinity for ATP more than its V_{max} decreases.

2.2. Myricetin inhibition of primase alone

The ability of myricetin to inhibit primase activity in the absence of DnaB was tested because it is an inhibitor of a variety of DNA polymerases, RNA polymerases, and reverse transcriptases.[38–41] This was also an important control for the more physiologically relevant reaction of DnaB-stimulated primer synthesis. When myricetin was added to the reaction containing primase and its substrates, it barely inhibited in a concentration-dependent manner (Fig. 3). It was not possible to test higher myricetin concentrations due to myricetin's low solubility. Even though the error in each measurement is about 5%, the same scale as the effect, fitting of the data to the inhibition equation revealed that the IC_{50} was 700 ± 300 μM myricetin. The consequence was that

Please cite this article in press as: Griep, M. A. et al., *Bioorg. Med. Chem.* (2007), doi:10.1016/j.bmc.2007.07.057

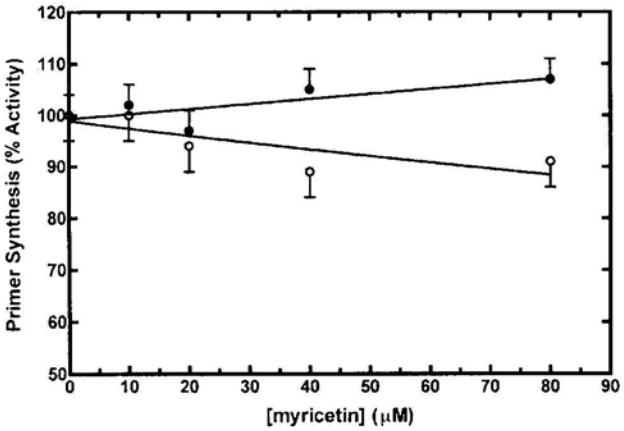

Figure 3. The effect of myricetin on *E. coli* primase activity in the presence (●) and absence (○) of *E. coli* DnaB helicase. Each data set was normalized to the number of primers synthesized in the absence of myricetin. In the absence of helicase, primase activity was weakly inhibited and poorly fit but the constants were $Y_{max} = 99 \pm 2\%$, $IC_{50} = 700 \pm 300$ μM myricetin, and an R^2 of 0.634. DnaB-stimulated primer synthesis could not be fit to a hyperbolic relationship so a line was drawn through the data to show the trend.

myricetin inhibited primase activity 60 times weaker than it inhibited DnaB ATPase activity and much weaker than the low micromolar IC_{50}'s for DNA polymerases, RNA polymerases, reverse transcriptases, and telomerases.[38–41] It may be relevant that the structure of bacterial primase differs from those palm-type nucleic acid polymerases in that it has a 'cashew-shaped' active site shared by no other polymerase family.[44,45]

2.3. Myricetin inhibition of DnaB-stimulated primer synthesis

Primase and DnaB stimulate each other's activities.[46] Of these cross-reactivities, the DnaB stimulation of primer synthesis activity is the most relevant to DNA replication because DNA polymerase cannot synthesize DNA without the resulting primer. Therefore, primer synthesis by primase was measured with and without helicase as a function of myricetin concentration. Unfortunately, the controls without myricetin but with DMSO showed that 0.5–4% DMSO, which would be added with 10–40 μM myricetin as its solvent, completely inhibited the helicase stimulation when it was present at its most stimulatory ratio relative to the primase.[12,13,46] This reduced level of primase activity was the same as primase alone and may reflect a slight stimulation effect by the myricetin (Fig. 3). Therefore, DMSO may not cause primase and helicase to dissociate from each other, but rather the presence of helicase may alter the ability of primase to be inhibited by myricetin.

3. Discussion

Myricetin is one of the six major flavonoids, plant pigments found in many foods and beverages, that are nutritionally interesting primarily for their antioxidant activities.[47] We show here that myricetin inhibits homohexameric *E. coli* DnaB with a K_i and IC_{50} of about 10 μM. The results also showed that myricetin would be an effective inhibitor at the log-phase-growth-phase ATP concentration of 3 mM.[48] The inhibitory mechanism was noncompetitive, indicating that myricetin does not bind to the active site. Even though the mechanism for ATP hydrolysis by hexameric helicases is complex, the current model for DnaB is that ATP can bind and be hydrolyzed in the active site of every other subunit.[49] Binding of ATP to the remaining three subunits is weaker and negatively cooperative.[50] For these reasons, it is interesting to speculate that myricetin is binding to the unfilled active sites to shut down the hydrolytic activity of the ATP-bound active sites.

The unwinding mechanism of the T7 gene 4 protein, a DnaB homolog, has been proposed to pass ssDNA from one subunit to another within the toroid as each adjacent subunit binds ATP, hydrolyzes it, and then releases ADP and phosphate.[51] When myricetin concentration is low, it must bind at or near the ATP pocket of one subunit such that it stimulates ATP synthesis in adjacent subunits. When myricetin concentration is moderate or high, it must bind to more than one subunit to lock the homohexamer into an inactive complex.

Other studies have shown that myricetin inhibited RSF1010 RepA, a distant hexameric helicase homolog, with a $K_i = 23$ μM and $IC_{50} = 50$ μM.[31] This is substantially weaker than the inhibition of DnaB helicase described here. The RepA myricetin inhibition kinetics also differed from those with DnaB in that they were competitive. Nevertheless, of the several flavonoids this group tested, myricetin was the most effective at inhibiting cellular growth. The minimal inhibitory concentration for *E. coli* was 0.50 mg/mL and for *Bacillus subtilis* was 0.25 mg/mL.[31]

RSF1010 RepA differs from both bacterial DnaB and T7 gene 4 protein in that it lacks a distinct N-terminal domain.[52,53] Specifically, DnaB is composed of three domains: the N-terminal domain (NTD or DnaBα), the ATPase shoulder (DnaBβ), and the C-terminal hexamerization domain (DnaBγ). Bacterial primase binds to the linker that connects the DnaB NTD with its ATPase domain.[54] Even though RepA interacts with RepC initiator protein and RepB′ primase, neither of those two enzymes is related by sequence to either *E. coli* DnaA or DnaG primase. Our results indicate that RSF1010 RepA is not a good model for DnaB perhaps because it lacks an N-terminal interaction domain.

There is only one crystal structure of inhibitory myricetin bound to one of its targets phosphatidylinositol-3-kinase (PIK3) (1E90.pdb).[55] Myricetin and 13 other flavonoids are low micromolar competitive inhibitors of PIK3, which is involved in signal transduction.[56] Given that they inhibited with similar affinities, it was remarkable to find that every one of the five co-crystallized flavonoids adopted a different orientation within the PIK3 ATP site. For instance, myricetin bound at a different angle than the structurally similar quercetin (1E8W.pdb). Nevertheless, since the ATPase sites of

Please cite this article in press as: Griep, M. A. et al., *Bioorg. Med. Chem.* (2007), doi:10.1016/j.bmc.2007.07.057

RepA and DnaB are smaller than the ATP binding site of PIK3, it should be possible to design compounds that fit more snugly into their active sites.

New and emerging pathogenic bacteria and the rise in multi-drug-resistant bacterial strains are driving the need to discover novel antibiotics. Only a few DNA replication enzymes are targets for current antibiotics. Bacterial primase and DnaB helicase are novel targets that are beginning to generate lead compounds from among natural products. In future studies, we will use structural models of the DnaB helicase active site to help engineer myricetin's structure to improve its selectivity and strength.

4. Materials and methods

4.1. Reagents

The *E. coli* DnaB helicase and primase were expressed and purified as described.[58,12] Ribonucleoside triphosphates (NTPs) were from Promega (Madison, WI). Myricetin, magnesium acetate, potassium glutamate, Hepes, and DTT were from Sigma (St. Louis, MO). Myricetin was dissolved in ethanol and its stock concentration determined using an extinction coefficient at 378 nm of 20,400 M^{-1} cm^{-1}.[59] It was then diluted into DMSO for use in the experiments.

4.2. Coupled ATPase assay

ATP hydrolysis by *E. coli* DnaB was measured by an NADH-coupled assay during which ATP was regenerated by the combined action of lactate dehydrogenase, pyruvate kinase, and their substrates.[60,61] The regeneration reaction caused the loss of one NADH for every ATP hydrolyzed in the primary reaction, such that ATP remained constant while NADH declined according to the ATPase activity of DnaB. NADH was continuously monitored at its absorption maximum of 340 nm, and its extinction coefficient plus stoichiometric factors were used to determine the moles ATP hydrolyzed per minute. The reaction buffer was 50 mM Hepes, 100 mM potassium glutamate, pH 7.5, 10 mM DTT, 400 μM NTPs, and 10 mM magnesium acetate.

4.3. Primer synthesis assay

Thermally denaturing HPLC analysis was used to determine the size, composition, and quantity RNA primers synthesized as previously described.[62] Briefly, RNA primer synthesis reactions were performed in 100 μl nuclease-free water reactions containing 50 mM HEPES, 100 mM potassium glutamate, pH 7.5, 10 mM DTT, 400 μM NTPs, and 10 mM magnesium acetate. DnaB helicase (800 nM hexamer) and ssDNA template (2 μM) were preincubated to the reaction temperature before the addition of primase (2 μM). HPLC purified synthetic ssDNA 23-mer with the sequence 5′-d(CAGACACACACACACTGCACACA)-3′ and with its 3′-end blocked by a C3 linker was obtained from Integrated DNA Technologies (Coralville, IA). *E. coli* primase initiates from the d(CTG) trinucleotide underlined in the template sequence. After incubation at 30 °C for 1 h, the samples were desalted through a Microspin G-25 column (Amersham, Piscataway, NJ) and then separated by thermally denaturing HPLC on a WAVE HPLC Nucleic Acid Fragment Analysis System with a DNASep HPLC column from Transgenomic (Omaha, NE).

4.4. Data-fitting

The data were fit to the indicated equations using Prism 4 for Macintosh (GraphPad Software, San Diego, CA).

Acknowledgment

This work was supported in part by a grant from the Department of Defense, Defense Advanced Research Program Agency (award W911NF0510275).

References and notes

1. Griep, M. A. Primase. In *Encyclopedia of Genetics*; Brenner, S., Miller, J., Eds.; Academic Press: New York, 2001.
2. Frick, D. N.; Richardson, C. C. *Annu. Rev. Biochem.* **2001**, *70*, 39.
3. Augustin, M. A.; Huber, R.; Kaiser, J. T. *Nat. Struct. Biol.* **2001**, *8*, 57.
4. Keck, J. L.; Berger, J. M. *Nat. Struct. Biol.* **2001**, *8*, 2.
5. Grompe, M.; Versalovic, J.; Koeuth, T.; Lupski, J. R. *J. Bacteriol.* **1991**, *173*, 1268.
6. Liu, J.; Dehbi, M.; Moeck, G.; Arhin, F.; Bauda, P.; Bergeron, D.; Callejo, M.; Ferretti, V.; Ha, N.; Kwan, T.; McCarty, J.; Srikumar, R.; Williams, D.; Wu, J. J.; Gros, P.; Pelletier, J.; DuBow, M. *Nat. Biotechnol.* **2004**, *22*, 185.
7. Zhang, Y.; Yang, F. D.; Kao, Y. C.; Kurilla, M. G.; Pompliano, D. L.; Dicker, I. B. *Anal. Biochem.* **2002**, *304*, 174.
8. Hegde, V. R.; Pu, H.; Patel, M.; Black, T.; Soriano, A.; Zhao, W.; Gullo, V. P.; Chan, T.-M. *Bioorg. Med. Chem. Lett.* **2004**, *14*, 2275.
9. Swart, J. R.; Griep, M. A. *Biochemistry* **1995**, *34*, 16097.
10. Khopde, S.; Biswas, E. E.; Biswas, S. B. *Biochemistry* **2002**, *41*, 14820.
11. Stayton, M. M.; Kornberg, A. *J. Biol. Chem.* **1983**, *258*, 13205.
12. Johnson, S. K.; Bhattacharyya, S.; Griep, M. A. *Biochemistry* **2000**, *39*, 736.
13. Bhattacharyya, S.; Griep, M. A. *Biochemistry* **2000**, *39*, 745.
14. Yoda, K.; Okazaki, T. *Mol. Gen. Genet.* **1991**, *227*, 1.
15. Schaeffer, P. M.; Headlam, M. J.; Dixon, N. E. *IUBMB Life* **2005**, *57*, 5.
16. Bonhoeffer, F.; Schaller, H. *Biochem. Biophys. Res. Commun.* **1965**, *20*, 93.
17. Bonhoeffer, F. *Z. Vererbungsl.* **1966**, *98*, 141.
18. Carl, P. L. *Mol. Gen. Genet.* **1970**, *109*, 107.
19. Sclafani, R. A.; Wechsler, J. A. *J. Bacteriol.* **1981**, *146*, 418.
20. Saluja, D.; Godson, G. N. *J. Bacteriol.* **1995**, *177*, 1104.
21. Masai, H.; Nomura, N.; Arai, K. *J. Biol. Chem.* **1990**, *265*, 15134.
22. Carr, K. M.; Kaguni, J. M. *J. Biol. Chem.* **2002**, *277*, 39815.

Please cite this article in press as: Griep, M. A. et al., *Bioorg. Med. Chem.* (2007), doi:10.1016/j.bmc.2007.07.057

23. Tougu, K.; Peng, H.; Marians, K. J. *J. Biol. Chem.* **1994**, *269*, 4675.
24. Gao, D. X.; McHenry, C. S. *J. Biol. Chem.* **2001**, *276*, 4441.
25. Shea, M. E.; Hiasa, H. *J. Biol. Chem.* **1999**, *274*, 22747.
26. Sivaraja, M.; Giordano, H.; Peterson, M. G. *Anal. Biochem.* **1998**, *265*, 22.
27. Earnshaw, D. L.; Pope, A. J. *J. Biomol. Screening* **2001**, *6*, 39.
28. Koepsell, S.; Hanson, S.; Hinrichs, S. H.; Griep, M. A. *Anal. Biochem.* **2005**, *339*, 353.
29. Chu, M.; Mierzwa, R.; Xu, L.; He, L.; Terracciano, J.; Patel, M.; Gullo, V.; Black, T.; Zhao, W.; Chan, T. M.; McPhail, A. T. *J. Nat. Prod.* **2003**, *66*, 1527.
30. Agarwal, A.; Louise-May, S.; Thanassi, J. A.; Podos, S. D.; Cheng, J.; Thoma, C.; Liu, C.; Wiles, J. A.; Nelson, D. M.; Phadke, A. S.; Bradbury, B. J.; Deshpande, M. S.; Pucci, M. J. *Bioorg. Med. Chem. Lett.* **2007**, 2807.
31. Xu, H.; Ziegelin, G.; Schroder, W.; Frank, J.; Ayora, S.; Alonso, J. C.; Lanka, E.; Saenger, W. *Nucleic Acids Res.* **2001**, *29*, 5058.
32. McKay, G. A.; Reddy, R.; Arhin, F.; Belley, A.; Lehoux, D.; Moeck, G.; Sarmiento, I.; Parr, T. R.; Gros, P.; Pelletier, J.; Far, A. R. *Bioorg. Med. Chem. Lett.* **2006**, *16*, 1286.
33. Leftheris, K.; Ahmed, G.; Chan, R.; Dyckman, A. J.; Hussain, Z.; Ho, K.; Hynes, J., Jr.; Letourneau, J.; Li, W.; Lin, S.; Metzger, A.; Moriarty, K. J.; Riviello, C.; Shimshock, Y.; Wen, J.; Wityak, J.; Wrobleski, S. T.; Wu, H.; Wu, J.; Desai, M.; Gillooly, K. M.; Lin, T. H.; Loo, D.; McIntyre, K. W.; Pitt, S.; Shen, D. R.; Shuster, D. J.; Zhang, R.; Diller, D.; Doweyko, A.; Sack, J.; Baldwin, J.; Barrish, J.; Dodd, J.; Henderson, I.; Kanner, S.; Schieven, G. L.; Webb, M. *J. Med. Chem.* **2004**, *47*, 6283.
34. Ong, K. C.; Khoo, H. E. *Gen. Pharmacol.* **1997**, *29*, 121.
35. Cushnie, T. P.; Lamb, A. J. *Int. J. Antimicrob. Agents* **2005**, *26*, 343.
36. McGovern, S. L.; Caselli, E.; Grigorieff, N.; Shoichet, B. K. *J. Med. Chem.* **2002**, *45*, 1712.
37. McGovern, S. L.; Helfand, B. T.; Feng, B.; Shoichet, B. K. *J. Med. Chem.* **2003**, *46*, 4265.
38. Shinozuka, K.; Kikuchi, Y.; Nishino, C.; Mori, A.; Tawata, S. *Experientia* **1988**, *44*, 882.
39. Ono, K.; Nakane, H.; Fukushima, M.; Chermann, J. C.; Barre-Sinoussi, F. *Eur. J. Biochem.* **1990**, *190*, 469.
40. Chu, S. C.; Hsieh, Y. S.; Lin, J. Y. *J. Nat. Prod.* **1992**, *55*, 179.
41. Menichincheri, M.; Ballinari, D.; Bargiotti, A.; Bonomini, L.; Ceccarelli, W.; D'Alessio, R.; Fretta, A.; Moll, J.; Polucci, P.; Soncini, C.; Tibolla, M.; Trosset, J. Y.; Vanotti, E. *J. Med. Chem.* **2004**, *47*, 6466.
42. Biswas, E. E.; Biswas, S. B. *Biochemistry* **1999**, *38*, 10929.
43. Biswas, E. E.; Biswas, S. B. *Biochemistry* **1999**, *38*, 10919.
44. Keck, J. L.; Roche, D. D.; Lynch, A. S.; Berger, J. M. *Science* **2000**, *287*, 2482.
45. Podobnik, M.; McInerney, P.; O'Donnell, M.; Kuriyan, J. *J. Mol. Biol.* **2000**, *300*, 353.
46. Koepsell, S. A.; Larson, M. A.; Griep, M. A.; Hinrichs, S. H. *J. Bacteriol.* **2006**, *188*, 4673.
47. Ross, J. A.; Kasum, C. M. *Annu. Rev. Nutr.* **2002**, *22*, 19.
48. Neuhard, J.; Nygaard, P. Purines and Pyrimidines. In *Escherichia coli and Salmonella typhimurium: Cellular and Molecular Biology*; Neihardt, F. C., Ed.; American Society for Microbiology: Washington, DC, 1987; Vol. 1, p 445.
49. Patel, S. S.; Picha, K. M. *Annu. Rev. Biochem.* **2000**, *69*, 651.
50. Bujalowski, W.; Klonowska, M. M. *Biochemistry* **1993**, *32*, 5888.
51. Liao, J. C.; Jeong, Y. J.; Kim, D. E.; Patel, S. S.; Oster, G. *J. Mol. Biol.* **2005**, *350*, 452.
52. Rawlings, D. E.; Tietze, E. *Microbiol. Mol. Biol. Rev.* **2001**, *65*, 481.
53. Weigel, C.; Seitz, H. *FEMS Microbiol. Rev.* **2006**, *30*, 321.
54. Thirlway, J.; Turner, I. J.; Gibson, C. T.; Gardiner, L.; Brady, K.; Allen, S.; Roberts, C. J.; Soultanas, P. *Nucleic Acids Res.* **2004**, *32*, 2977.
55. Walker, E. H.; Pacold, M. E.; Perisic, O.; Stephens, L.; Hawkins, P. T.; Wymann, M. P.; Williams, R. L. *Mol. Cell* **2000**, *6*, 909.
56. Agullo, G.; Gamet-Payrastre, L.; Manenti, S.; Viala, C.; Remesy, C.; Chap, H.; Payrastre, B. *Biochem. Pharmacol.* **1997**, *53*, 1649.
57. Xu, H.; Frank, J.; Niedenzu, T.; Saenger, W. *Biochemistry* **2000**, *39*, 12225.
58. Griep, M. A.; Lokey, E. R. *Biochemistry* **1996**, *35*, 8260.
59. Mira, L.; Fernandez, M. T.; Santos, M.; Rocha, R.; Florencio, M. H.; Jennings, K. R. *Free Radic. Res.* **2002**, *36*, 1199.
60. Rosing, J.; Harris, D. A.; Kemp, A., Jr.; Slater, E. C. *Biochim. Biophys. Acta* **1975**, *376*, 13.
61. Harris, D. A. Spectrophotometric Assays. In *Spectrophotometry & Spectrofluorimetry: A Practical Approach*; Harris, D. A., Bashford, C. L., Eds.; IRL Press: Oxford, 1988.
62. Koepsell, S.; Bastola, D.; Hinrichs, S. H.; Griep, M. A. *Anal. Biochem.* **2004**, *332*, 330.

Please cite this article in press as: Griep, M. A. et al., *Bioorg. Med. Chem.* (2007), doi:10.1016/j.bmc.2007.07.057